DEPARTMENT OF ENGINEERING SCIENCE AND MECHANICS
VIRGINIA POLYTECHNIC INSTITUTE AND STATE UNIVERSITY
BLACKSBURG, VIRGINIA
AND
DEPARTMENT OF MECHANICAL ENGINEERING AND MECHANICS
OLD DOMINION UNIVERSITY
NORFOLK, VIRGINIA

INVESTIGATIONS INTO THE MECHANICAL BEHAVIOR

OF COMPOSITE BOLTED JOINTS

J. C. Perry

and

M. W. Hyer

Principal Investigator: Earl A. Thornton

Interim Report
For the period June 1978 - March 1979

Prepared for the
National Aeronautics and Space Administration
Langley Research Center
Hampton, Virginia

June 1979

DEPARTMENT OF ENGINEERING SCIENCE AND MECHANICS
VIRGINIA POLYTECHNIC INSTITUTE AND STATE UNIVERSITY
BLACKSBURG, VIRGINIA
AND
DEPARTMENT OF MECHANICAL ENGINEERING AND MECHANICS
OLD DOMINION UNIVERSITY
NORFOLK, VIRGINIA

INVESTIGATIONS INTO THE MECHANICAL BEHAVIOR

OF COMPOSITE BOLTED JOINTS

By
J. C. Perry

and

M. W. Hyer

Principal Investigator: Earl A. Thornton

TABLE OF CONTENTS

LIST OF TABLES

Preceding page blank

LIST OF FIGURES

LIST OF FIGURES (CONCL'D)

ABSTRACT

This report summarizes the results of two studies which had as a primary purpose the determination of the load-carrying capacity of composite bolted joints. The first study was actually a pilot program designed to establish testing procedures, data reduction, and data interpretation for a larger, long-term program. The purpose of the overall program was to study the mechanical behavior of bolted joints at room temperature, -157° C (-250° F), and 315° C (600° F). The second part of the study investigated the load transfer characteristics, from one bolt to another, in double-bolt joints by examining data generated in previous investigations. From the results, it appears the increase in load-carrying capacity by adding a second bolt in tandem can be predicted.

INVESTIGATIONS INTO THE MECHANICAL BEHAVIOR OF COMPOSITE BOLTED JOINTS

By

J. C. Perry[1] and M. W. Hyer[2]

INTRODUCTION

Bolted joints appear to be an attractive method for the interconnection of structural components fabricated from fiber-reinforced composite materials. This is particularly true if replacement and repair of components is required during the life of the structure. With the alternative connection methods, namely adhesive-bonding and integral construction, wholesale refabrication may be necessary if the replacement of a single component is required. Work has been done on joints intended for both primary and secondary structures (refs. 1 to 3). This report covers the continued investigation into bolted joints and consists essentially of two parts. The first part deals with the testing of bolted joints under conditions of extreme temperature environments, and the second part deals with analyses of past data to determine the load transfer characteristics in joints with more than one bolt.

ENVIRONMENTAL TESTING OF BOLTED JOINT SPECIMENS

This portion of the research effort was actually a pilot project for a much larger effort which had as its objective the comparing of the mechanical behavior of bolted joint specimens from two different manufacturers. The objectives of the pilot project were to (1) set up the experimental equipment and establish the procedures for testing of graphite-polyimide bolted joint specimens at -157° C (-250° F), room temperature (RT), and 315° C (600° F), (2) actually test a preliminary sample of specimens, and (3) establish a data-reduction/data-interpretation procedure. This preliminary project was conducted with specimens which were identical in design to those to be tested

---

[1] Research Assistant, Old Dominion University Research Foundation, P.O. Box 6369, Norfolk, Virginia 23508.

[2] Assistant Professor, Department of Engineering Science and Mechanics, Virginia Polytechnic Institute and State University, Blacksburg, Virginia 24061.

in the overall project. The primary purposes of the first and second objectives were to determine the load range, failure mode, and load-deflection characteristics of the specimens. In addition, knowledge of heat-up/cool-down times, temperature gradients, and potential defects in the test equipment were necessary in order to better plan the overall project. It was with the preliminary specimens that the three objectives of this pilot project were studied.

TEST CHAMBER SETUP

The environmental chamber used was an Applied Test System Series 2912 barrel-type chamber. The chamber allows tensile testing of specimens in a high or low temperature environment. Considerable effort was involved in positioning the specimens axially in the environmental test chamber so that the temperature gradients were minimized in the region around the test-hole in the specimen. For the high and low temperature tests, one specimen design was used, while for the RT testing a second design was used. Figures 1 and 2 show the designs. There were two designs mainly because it was desirable to have the aluminum load transfer doublers on the specimens out of the temperature extremes of the central portion of the test chamber. Differences in the coefficient of thermal expansion between the aluminum and graphite/polyimide could have been detrimental to the doubler adhesive bond, so this region of the test specimen was kept away from the temperature extremes.

In addition to the thermocouple which measured the air temperature inside the test chamber, five thermocouples were mounted on the specimen to measure specimen temperature in the vicinity of the test hole. After several adjustments to attain the correct axial position in the oven, the specimen had a satisfactory temperature distribution in the test hole area. Figure 3 shows the temperature distribution for the high and low temperature test conditions. The thermocouples were held against the test specimen with metal clips. Pieces of mica were used to insulate the thermocouples against any heat-sink effects of the metal clips.

MEASUREMENT OF SPECIMEN RESPONSE

It would be of immense value if the stress and/or strain distribution around the holes in loaded joints could be measured. Unfortunately, due to

2

the high strain gradients near the hole, strain gages cannot accurately measure the response of the material (ref. 4). In addition, the bolt heads are too large to allow mounting of a strain gage close to the hole. Thus, alternative methods of measuring the response are necessary. For these tests, it was felt load-deflection characteristics of the joints might be of some value. The character of the load-deflection trace together with visual examination of the failed specimen perhaps would prove valuable in assessing the failure mode. A linear-variable-differential-transformer (LVDT) was mounted so as to measure change in distance between the loading heads of the test machine. The head displacement was then plotted as a function of load with an online x-y plotter, and the characteristics of the x-y relationship from no-load to failure were then studied. The relations were studied for the range of linearity, initial slope, maximum load and the response between the end of the linear region and the maximum load. Figures 4 and 5 show typical load-deflection relations. The methodology for analyzing the curves was as follows: first the initial slope was drawn by visual examination of the curve. Second, the point on the trace corresponding to the end of the linear region was noted. This point described the end of linear material behavior. If the joint material had been metal, yield would have begun shortly after this point. In figure 4 this point has a load value of 8450 N (1900 lb), while in figure 5 the value is 9120 N (2050 lb). From the closeness of these two values, it can be said the two specimens behaved similarly in the linear region when under the same environmental conditions. The type of failure mode is indicated by the behavior of the curve beyond the linear region. A small additional displacement after the end of the linear region, combined with a sharp dropoff in load after the maximum load was reached, seemed to indicate a failure in net-section tension. If after the linear range there was a large amount of displacement, combined with several small drops in load, the joint most likely failed in bearing. Using these criteria, figure 4 represents a net-section tension failure and figure 5 represents a bearing failure. This graphical approach was applied to note any possible trends in the type of failure as a function of specimen geometry or test temperature. It was just one approach to the data analysis, and other methods were needed.

As another approach to data reduction and interpretation, and for better understanding of the relationship between the failure stress and parameters

such as strip width (W), bolt diameter (D), distance of the bolt from the
end of the specimen (e), and test temperature, the experimental data and
analysis techniques of other investigators (refs. 1 to 3) were studied. The
analysis of data in reference 1 was felt to be the most useful. In that
investigation, the bearing stress at failure and the net section tensile
stress at failure were plotted as a function of the dimensionless ratio W/D.
It was felt those plots were useful and should be applied in the present
situation. In order to simplify the data reduction process, a computer
program was written to do the computations. The program used the failure
load and specimen geometry to generate tensile and bearing shearout stress,
in addition to the dimensionless ratios W/D and e/D. Table 1 is the output
of the computer program and shows the results of all tests using the pre-
liminary specimens.

To further aid in the data reduction, the use of an existing interactive
graphics computer program (ref. 5) was felt to have some advantages. This
program performs least-squares statistical analysis with a variety of graphic
display options. Using the program, several types of plots, using the test
data, were generated. These are explained below.

Figure 6 shows the bearing stress at failure vs. W/D for the 4 specimens
tested at 315° C (600° F). Figures 7 and 8 show the data with first order
and second order polynomials, respectively, statistically faired through
the data points. Figure 9 shows the net-section tensile stress at failure
vs. W/D for those same four specimens with a first-order polynomial passing
through the data. The failure modes are mixed so the data isn't totally
consistent. However, the trend is similiar to those seen in reference 1.
Data at the other two test temperatures, -157° C (-250° F) and RT, showed
similiar trends, but not all the data showed as smooth a trend. This was felt
to be due to the small sample size and perhaps not representative of a physical
trend. However, this exercise was not so much to generate hard data and
trends as it was to establish tools for data reduction. The two computer
programs used are felt to be useful tools for the analysis of large amounts
of data and, in particular, the interactive program could be used for
convenient display and statistical analysis of the data.

4

LOAD TRANSFER IN COMPOSITE BOLTED JOINTS

The second portion of the study dealt with the effect of using two bolts
in tandem, as opposed to a single bolt, to transfer the load from one portion
of the joint to the other. Conceptually, two bolts might be better than one,
and three might be better than two, but of course the joint weight increases
and the overlap is longer. For metal joints, if the stress around one bolt
hole exceeds yield, the material deforms and transfers part of the load to
the other bolt or bolts. For composites, with their brittle-like material
behavior, this transfer-through-yielding will not take place in exactly the
same way. Failure always seems to occur at the leading bolt (refs. 2 to 3)
and so the question arises as to the value of a second bolt in tandem. In
references 6 and 7, the approach to designing graphite-epoxy joints with
multiple bolts was as follows: A single-bolt must react 100 percent of the
load and bypass 0 percent, whereas an open-hole (no bolt) bypasses 100 per-
cent of the load and reacts 0 percent. The load capacity of a two-bolt joint
was assumed to be the capacity of the single-bolt plus one-half the difference
between the open-hole and the single bolt. Alternatively, the load capacity
of a double-bolt joint was assumed to be the average of the single-bolt load
and the open-hole load. The experimental results of references 6 and 7 show
this trend in the experimental data. The question is whether this trend is
evident in other test data. The preliminary specimens used to set up the
test chamber and to generate initial failure information were not of suffi-
cient quantity to perhaps demonstrate this trend. Thus, data from other
sources was examined, in particular, the data of reference 2. The experi-
mental data from that report was rearranged so open-hole, single-hole, and
double-hole specimens were grouped by hole diameter and W/D. In addition,
the grouping was done according to the series A testing and series B testing
of that reference. The specimens used in reference 2 were similar in design
to the specimen design of figure 2, namely four test holes per specimen.
In reference 2, series A testing refers to testing the outer two holes, left
and right, and series B testing refers to testing the holes closest to the
central aluminum doublers. It was demonstrated (ref. 3) the failure loads
of the series B tests were significantly different, i.e., statistically
significant, by several percent, than the failure loads of the series A
tests.

After this grouping, an average was taken of the net-section failure stress for each type of specimen, i.e., for the open-hole, single-hole, and double-hole specimens. Then a failure load, based on the average of the open-hole and single-hole data, was predicted for the double-hole specimens. This predicted value was compared with the actual load and a percent error calculated. The results are shown in tables 2 through 13. Each table presents the results from a particular hole size and W/D ratio.

From the tables it can be seen the predictions for double-hole specimens agreed quite well with the actual results. In the worst case, the predictions were 12 percent different than the actual value. It should be pointed out, however, that for a given geometry, the difference between open-hole and single-hole failure loads was as low as 15 percent [hole = 11.1 mm (0.438 in.) diameter; W/D = 4] of the average of the two values. Thus, it was the average of two numbers not radically different which was predicted, and close agreement could have been expected. Figures 10 through 33 show the data from these tables plotted with a least-squares straight line (since averaging is a straight-line approximation) faired through the data. On the horizontal axis is the percent load transfer assuming the open-hole has 0 percent transmitted to the bolt, the single-hole has 100 percent transmitted to the bolt, and the double-hole has 50 percent transmitted. On the vertical axis is the net-section tensile stress at failure for the three specimen types. Figures 10 through 21 show the raw data, while figures 22 through 33 show the averaged data.

From that data, several conclusions are evident:

(1) the actual double-hole joint values for the load-carrying capacity are close to the predicted 50 percent load transfer;

(2) for a fixed diameter, the net-section tension failure stress for each type of specimen decreases with increasing W/D;

(3) the decrease in value of the net-section stress is much greater for the single-hole joints than for the open-hole specimens or the two-hole joints; and

(4) the decrease in net-section tension for increasing W/D is smallest for the open-hole specimens.

It is the first observation that is significant, since it was such a trend that was being sought. For the cryogenic and high-temperature testing, it would be informative to know if this same load transfer trend is present. As a result of the trends observed in this study, open-hole specimens have been added to the test program which had originally included only single- and double-hole joints.

ACKNOWLEDGMENTS

8

REFERENCES

1. Hart-Smith, L.J.: Bolted Joints in Graphite Epoxy Composites. McDonnell-Douglas Corp., NASA CR-144899, June 1976.

2. Hyer, M.W.; and Lightfoot, M.C.: Composite Bolted-Joint Specimens: Experimental Results. NASA CR-158964, Nov. 1978.

3. Hyer, M.W.; and Lightfoot, M.C.: Ultimate Strength of High-Load Capacity Composite Bolted Joints. ASTM 5th Conference on Composite Materials: Testing and Design, STP 674, June 1979.

4. Hyer, M.W.; and Lightfoot, M.C.: Strain Measurements in Composite Bolted Joint Specimens. NASA Report, Grant NSG 1167, May 1979.

5. Lightfoot, M.C.; and Hyer, M.W.: GILSA: General Interactive Least-Squares Analysis. Progress Report for NASA Grant NSG 1167, Aug. 1978.

6. Whitman, B.; Shyprykervich, P.; and Whiteside, J.: Design of the B-1 Composite Horizontal Stabilizer Root Joint. NASA TM X-3377. Third Conference on Fibrous Composites in Flight Vehicle Design, Apr. 1976.

7. Johnson, R.W.; and McCarty, J.E.: Design and Fabrication of Graphite-Epoxy Bolted Wing Skin Splice Specimens. The Boeing Commercial Airplane Co., NASA CR-145216, May 1977.

Table 1. Test results of preliminary specimens (computer program output).

TEST TEMP (°C)	W/D	e/D	FAILURE LOAD (N)	TENSILE STRESS (MPa)	BEARING STRESS (MPa)	SHEAROUT STRESS (MPa)	FAILURE LOAD
21.	3.998	3.034	11819.	276.	828.	164.	NET-TENSION
21.	4.005	3.013	11432.	264.	792.	157.	NET-TENSION
21.	4.992	3.034	12566.	220.	883.	175.	NET-TENSION-COM
21.	5.005	3.029	12522.	212.	834.	166.	NET-TENSION
21.	6.011	3.025	12233.	171.	867.	172.	BEARING
21.	6.011	1.971	14946.	200.	999.	144.	BEARING
21.	4.002	4.035	12900.	297.	876.	124.	NET-TENSION
21.	4.004	4.074	11966.	274.	812.	114.	NET-TENSION
21.	4.995	1.075	13812.	238.	949.	133.	BEARING-TENSION
21.	5.003	4.026	12455.	215.	846.	123.	BEARING-TENSION
21.	6.011	4.105	14301.	199.	995.	139.	BEARING
21.	6.011	3.103	12477.	174.	844.	164.	BEARING
318.	5.029	4.033	10453.	184.	766.	109.	BEARING
316.	4.054	3.030	10298.	227.	691.	137.	NET-TENSION
319.	4.020	4.033	9697.	237.	730.	103.	NET-TENSION
318.	6.026	3.986	10453.	146.	778.	112.	BEARING
-158.	4.036	3.028	11921.	296.	924.	183.	NET-TENSION
-159.	4.021	4.041	12455.	279.	837.	119.	NET-TENSION
-159.	6.021	3.986	14813.	210.	1096.	158.	BEARING

Table 2. Predicted vs. actual net-section failure stress for double-hole specimens, group A1, in MPa (ksi); D = 11.1 mm (0.438 in.); W/D = 4.

Actual			Predicted Double-Hole Failure Stress	Percent Error in Prediction
Open-Hole Specimen No.: Failure Stress	Single-Hole Specimen No.: Failure Stress	Double-Hole Specimen No.: Failure Stress		
OH-1L: 303 (43.9)	DLSH-1L: 246 (35.7)	DLDH-1: 286 (41.5)	Predicted = Single-Hole + $\frac{1}{2}$ (Open-Hole Minus Single-Hole)	
OH-2L: 290 (42.1)	DLSH-7L: 242 (35.1)	DLDH-2: 296 (43.0)		
OH-1R: 283 (41.0)	DLSH-8L: 235 (34.1)	DLDH-18: 271 (39.3)		
OH-2R: 293 (42.5)	DLSH-1R: 272 (39.4)			
	DLSH-7R: 245 (35.5)			
	DLSH-8R: 243 (35.2)			
Average: 292 (42.4)	252 (36.5)	285 (41.3)	272 (39.5)	4.3 (low)

Table 3. Predicted vs. actual net-section failure stress for double-hole specimens, group A2, in MPa (ksi); D = 11.1 mm (0.438 in.); W/D = 6.

Actual			Predicted Double-Hole Failure Stress	Percent Error in Prediction
Open-Hole Specimen No.: Failure Stress	Single-Hole Specimen No.: Failure Stress	Double-Hole Specimen No.: Failure Stress		
OH-3L: 275 (39.9)	DLSH-2L: 196 (28.4)	DLDH-3: 234 (34.0)	Predicted =	
OH-4L: 275 (39.9)	DLSH-2R: 179 (26.0)	DLDH-4: 243 (35.2)	Single-Hole + $\frac{1}{2}$ (Open-Hole	
OH-3R· 278 (40.4)		DLDH-19: 213 [a] (30.9)	Minus Single-	
OH-4R: 277 (40.2)		DLDH-20: 214 [a] (31.1)	Hole)	
Average: 276 (40.1)	188 (27.2)	238 (34.6)	232 (33.6)	2.9 (low)

[a] Failed in doubler area, essentially a single-hole failure, not included in computation of average.

Table 4. Predicted vs. actual net-section failure stress for double-hole specimens, group A3, in MPa (ksi); D = 11.1 mm (0.438 in.); W/D = 8.

Actual			Predicted Double-Hole Failure Stress	Percent Error in Prediction
Open-Hole Specimen No.: Failure Stress	Single-Hole Specimen No.: Failure Stress	Double-Hole Specimen No.: Failure Stress		
OH-5L: 286 (41.5)	DLSH-3L: 144 (20.9)	DLDH-5: 165[a] (24.0)	Predicted = Single-Hole + $\frac{1}{2}$ (Open-Hole Minus Single-Hole)	
OH-6L: 270 (39.2)	DLSH-9L: 120 (17.4)	DLDH-6: 156[a] (27.7)		
OH-5R: 276 (40.1)	DLSH-3R: 131 (19.0)	DLDH-7: 211 (30.6)		
OH-6R: 278 (40.4)	DLSH-9R: 126 (18.3)	DLDH-8: 221 (32.0)		
		DLDH-21: 175 (25.4)		
		DLDH-22: 123[b] (17.9)		
Average 278 (40.3)	130 (18.9)	202 (29.3)	204 (29.6)	1 (high)

[a] Specimens tested at McDonnell-Douglas Aircraft Corp. (MDAC), failure reported to be bearing, not included in computation of average.

[b] Failed in doubler area, essentially a single-hole failure, not included in computation of average.

14

Table 5. Predicted vs. actual net-section failure stress for double-hole specimens, group A4, in MPa (ksi); D = 15.9 mm (0.625 in.); W/D = 4.

Actual			Predicted Double-Hole Failure Stress	Percent Error in Prediction
Open-Hole Specimen No.: Failure Stress	Single-Hole Specimen No.: Failure Stress	Double-Hole Specimen No.: Failure Stress		
OH-7L: 288 (41.8)	DLSH-4L: 222 (32.2)	DLDH-9: 272 (39.5)	Predicted = Single-Hole + $\frac{1}{2}$ (Open-Hole Minus Single-Hole)	
OH-8L: 304 (44.1)	DLSH-10L: 218 (31.7)	DLDH-10: 259 (37.6)		
OH-7R: 282 (40.9)	DLSH-4R: 226 (32.8)	DLDH-23: 256 (37.2)		
OH-8R: 293 (42.5)	DLSH-10R: 214 (31.0)	DLDH-24: 250 (36.3)		
Average: 292 (42.3)	220 (31.9)	259 (37.6)	256 (37.1)	1.3 (low)

Table 6. Predicted vs. actual net-section failure stress for double-hole specimens, group A5, in MPa (ksi); D = 15.9 mm (0.625 in.); W/D = 6.

Actual			Predicted Double-Hole Failure Stress	Percent Difference
Open-Hole Specimen No.: Failure Stress	Single-Hole Specimen No.: Failure Stress	Double-Hole Specimen No.: Failure Stress		
OH-9L: 266 (38.6)	DLSH-5L: 154 (22.4)	DLDH-11: 224 (32.5)	Predicted =	
OH-10L: 271 (39.3)	DLSH-11L: 145 (21.0)	DLDH-12: 216 (31.3)	Single-Hole + $\frac{1}{2}$ (Open-Hole	
OH-9R: 265 (38.4)	DLSH-5R: 168 (24.4)	DLDH-26: 168 [a] (24.3)	Minus Single-	
OH-10R: 267 (38.7)	DLSH-11R: 144 (20.9)		Hole)	
Average: 268 (38.8)	153 (22.2)	220 (31.9)	210 (30.5)	4.4 (low)

[a] Failed in doubler area, essentially a single-hole failure, not included in computation of average.

Table 7. Predicted vs. actual net-section failure stress for double-hole specimens, group A6, in MPa (ksi); D = 15.9 mm (0.625 in.); W/D = 8.

Actual			Predicted Double-Hole Failure Stress	Percent Error in Prediction
Open-Hole Specimen No.: Failure Stress	Single-Hole Specimen No.: Failure Stress	Double-Hole Specimen No.: Failure Stress		
OH-11L: 248 (36.0)	DLSH-6L: 121 (17.6)	DLDH-13: 194[a] (28.2)	Predicted =	
OH-12L: 254 (36.8)	DLSH-12L: 106 (15.4)	DLDH-14: 192 (27.8)	Single-Hole +	
OH-11R: 258 (37.5)	DLSH-6R: 121 (17.5)	DLDH-15: 128[b] (18.5)	$\frac{1}{2}$ (Open-Hole	
OH-12R: 257 (37.3)	DLSH-12R: 108 (15.7)	DLDH-16: 208[b] (30.1)	Minus Single-Hole)	
		DLDH-27: 170 (24.6)		
		DLDH-28: 169 (24.5)		
		DLDH-29: 170[c] (24.6)		
		DLDH-30: 170[c] (24.6)		
Average: 254 (36.9)	114 (16.6)	170 (24.6)	185 (26.8)	8.9 (low)

[a] Outer laps curled, washers on bolt dug into laminate, not included in computation of average.

[b] Tested at MDAC, failure reported to be bearing, not included in computation of average.

[c] Tested at MDAC, failure reported to be tensile, included in computation of average.

Table 8. Predicted vs. actual net-section failure stress for double-hole specimens, group B1, in MPa (ksi); D = 11.1 mm (0.438 in.); W/D = 4.

Actual			Predicted Double-Hole Failure Stress	Percent Error in Prediction
Open-Hole Specimen No.: Failure Stress	Single-Hole Specimen No.: Failure Stress	Double-Hole Specimen No.: Failure Stress		
OH-1L: 303 (43.9)	DLSH-1L: 260 (37.7)	DLDH-1: 286 (41.5)	Predicted =	
OH-2L: 290 (42.1)	DLSH-7L: 241 (35.0)	DLDH-2: 296 (43.0)	Single-Hole +	
OH-1R: 283 (41.0)	DLSH-8L: 241 (35.0)	DLDH-18: 271 (39.3)	$\frac{1}{2}$ (Open-Hole Minus Single-Hole)	
OH-2R: 293 (42.5)	DLSH-1R: 263 (38.1)			
	DLSH-7R: 241 (35.0)			
Average: 292 (42.4)	250 (36.2)	285 (41.3)	271 (39.3)	4.8 (low)

17

Table 9. Predicted vs. actual net-section failure stress for double-hole specimens, group B2, in MPa (ksi); D = 11.1 mm (0.438 in.); W/D = 6.

Actual			Predicted Double-Hole Failure Stress	Percent Error in Prediction
Open-Hole Specimen No.: Failure Stress	Single-Hole Specimen No.: Failure Stress	Double-Hole Specimen No.: Failure Stress		
OH-3L: 275 (39.9)	DLSH-2L: 220 (31.9)	DLDH-3: 234 (34.0)	Predicted = Single-Hole + $\frac{1}{2}$ (Open-Hole Minus Single-Hole)	
OH-4L: 275 (39.9)	DLSH-2R: 227 (33.0)	DLDH-4: 243 (35.2)		
OH-3R: 278 (40.4)		DLDH-19: 213[a] (30.9)		
OH-4R: 277 (40.2)		DLDH-20: 214[a] (31.1)		
Average: 276 (40.1)	223 (32.4)	238 (34.6)	250 (36.2)	4.6 (high)

[a] Failed in doubler area, essentially a single-hole failure, not included in computation of average.

Table 10. Predicted vs. actual net-section failure stress for double-hole specimens, group B3, in MPa (ksi); D = 11.1 mm (0.438 in.); W/D = 8.

Actual			Predicted Double-Hole Failure Stress	Percent Error in Prediction
Open-Hole Specimen No.: Failure Stress	Single-Hole Specimen No.: Failure Stress	Double-Hole Specimen No.: Failure Stress		
OH-5L: 286 (41.5)	DLSH-3L: 159 (23.0)	DLDH-5: 165[a] (24.0)	Predicted = Single-Hole + $\frac{1}{2}$ (Open-Hole Minus Single-Hole)	
OH-6L: 270 (39.2)	DLSH-9L: 154[c] (22.3)	DLDH-6: 156[a] (22.7)		
OH-5R: 276 (40.1)	DLSH-3R: 159 (23.1)	DLDH-7: 211 (30.6)		
OH-6R: 278 (40.4)		DLDH-8: 221 (32.0)		
		DLDH-21: 175 (25.4)		
		DLDH-22: 123[c] (17.9)		
Actual: 278 (40.3)	158 (23.0)	202 (29.3)	218 (31.6)	7.8 (high)

[a] Specimen tested at MDAC, failure reported to be bearing, not included in computation of average.

[b] Doubler disbond, not included in computation.

[c] Failed in doubler area, essentially a single-hole failure, not included in computation of average.

Table 11. Predicted vs. actual net-section failure stress for double-hole specimens, group B4, in MPa (ksi); D = 15.9 mm (0.625 in.); W/D = 4.

Actual			Predicted Double-Hole Failure Stress	Percent Difference
Open-Hole Specimen No.: Failure Stress	Single-Hole Specimen No.: Failure Stress	Double-Hole Specimen No.: Failure Stress		
OH-7L: 288 (41.8)	DLSH-4L: 225 (32.7)	DLDH-9: 272 (39.5)	Predicted =	
OH-8L: 304 (44.1)	DLSH-10L: 218 (31.6)	DLDH-10: 259 (37.6)	Single-Hole + $\frac{1}{2}$ (Open-Hole	
OH-7R: 282 (40.9)	DLSH-4R: 231 (33.5)	DLDH-23: 256 (37.2)	Minus Single-	
OH-8R: 293 (42.5)	DLSH-10R: 214 (31.0)	DLDH-24: 250 (36.3)	Hole)	
Average: 292 (42.3)	222 (32.2)	259 (37.6)	256 (37.2)	1 (low)

Table 12. Predicted vs. actual net-section failure stress for double-hole specimens, group B5, in MPa (ksi); D = 15.9 mm (0.625 in.); W/D = 6.

Actual			Predicted Double-Hole Failure Stress	Percent Error in Prediction
Open-Hole Specimen No.: Failure Stress	Single-Hole Specimen No.: Failure Stress	Double-Hole Specimen No.: Failure Stress		
OH-9L: 266 (38.6)	DLSH-5L: 163 (23.7)	DLDH-11: 224 (32.5)	Predicted = Single-Hole + $\frac{1}{2}$ (Open-Hole Minus Single-Hole)	
OH-10L: 271 (39.3)	DLSH-11L: 154 (22.3)	DLDH-12: 216 (31.3)		
OH-9R: 265 (38.4)	DLSH-5R: 184 (26.7)	DLDH-26: 168[a] (24.3)		
OH-10R: 267 (38.7)	DLSH-11R: 159 (23.1)			
Average: 268 (38.8)	165 (24.0)	220 (31.9)	216 (31.4)	1.6 (low)

[a] Failed in doubler area, essentially a single-hole failure, not included in computation of average.

Table 13. Predicted vs. actual net-section failure stress for double-hole specimens, group B6, in MPa (ksi); D = 15.9 mm (0.625 in.); W/D = 8.

Actual			Predicted Double-Hole Failure Stress	Percent Error in Prediction
Open-Hole Specimen No.: Failure Stress	Single-Hole Specimen No.: Failure Stress	Double-Hole Specimen No.: Failure Stress		
OH-11L: 248 (36.0)	DLSH-6L: 128 (18.5)	DLDH-13: 194[a] (28.2)	Predicted = Single-Hole + $\frac{1}{2}$ (Open-Hole Minus Single-Hole)	
OH-12L: 254 (36.8)	DLSH-12L: 121 (17.5)	DLDH-14: 192 (27.8)		
OH-11R: 258 (37.5)	DLSH-6R: 134 (19.5)	DLDH-15: 128[b] (18.5)		
OH-12R: 257 (37.3)	DLSH-12R: 116 (16.9)	DLDH-16: 208[b] (30.1)		
		DLDH-27: 170 (24.6)		
		DLDH-28: 169 (24.5)		
		DLDH-29: 170[c] (24.7)		
		DLDH-30: 170[c] (24.6)		
Average: 254 (36.9)	125 (18.1)	170 (24.6)	190 (27.5)	11.8 (high)

[a] Outer laps curled, washers on bolt dug into laminate, not included in computations of average.

[b] Tested at MDAC, failure reported to be bearing, not included in computation of average.

[c] Tested at MDAC, failure reported to be tensile, included in computation of average.

ALUMINUM DOUBLERS

16 PLIES GRAPHITE/POLYIMIDE
(QUASI-ISOTROPIC)

2.29 (0.090)

2.50 (0.098)

203
(8.00)

38.1
(1.50)

19.0
(0.750)

14.7
(0.580)

12.7
(0.50)

25.4
(1.00)

6.35 (0.250) DIA.

TEST HOLE
0.76 (0.188) DIA.
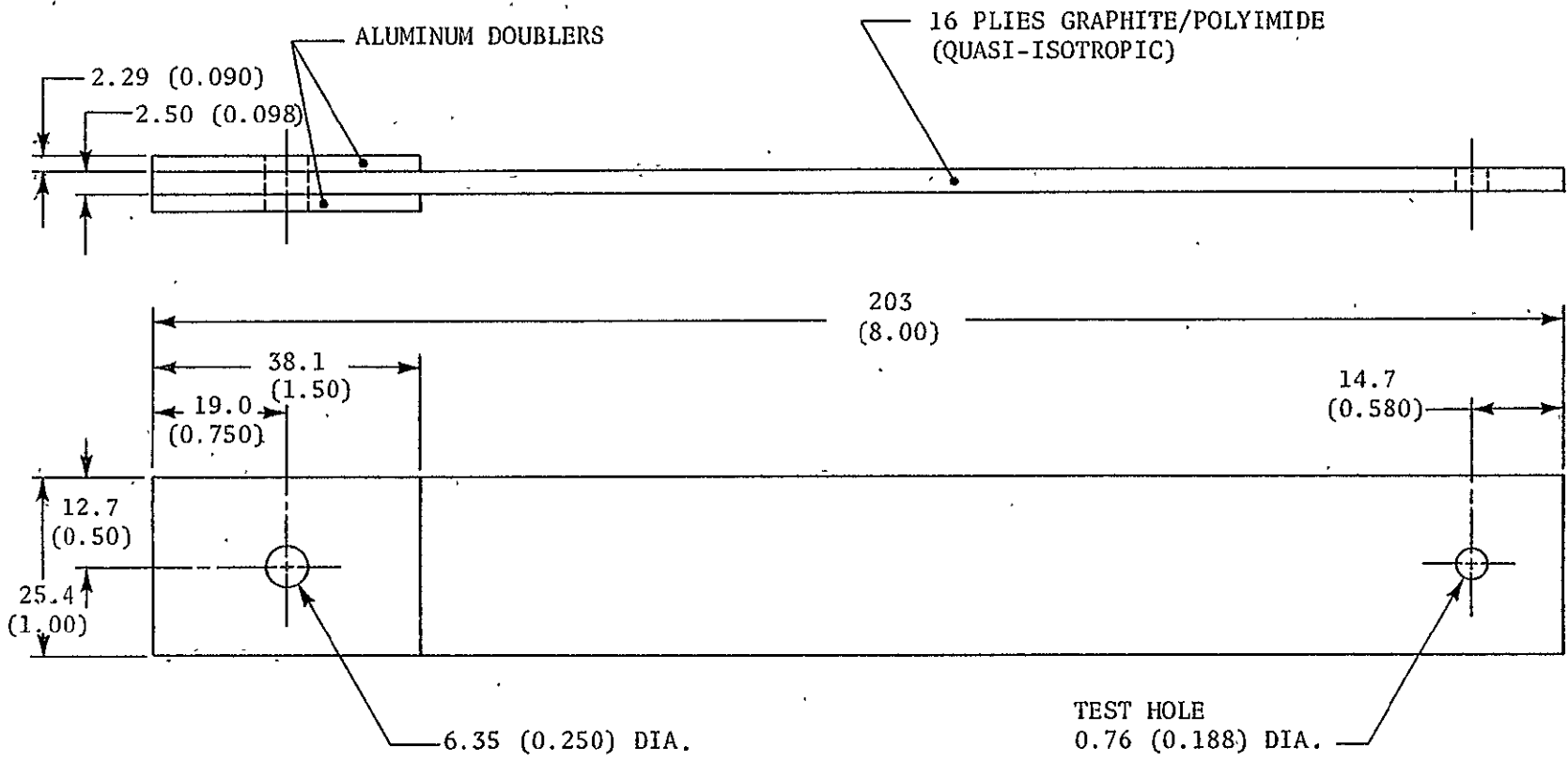
Figure 1.   Specimen design for high and low temperature tests
[dimensions in mm (in.)].

ALUMINUM DOUBLERS

16 PLIES GRAPHITE/POLYIMIDE
(QUASI-ISOTROPIC)

2.50
(0.098)

2.39
(0.090)

178
(7.00)

88.9
(3.50)

14.7
(0.580)

44.4
(1.75)

10.0
(0.394)

20.0
(0.787)

38.1
(1.50)

4 TEST HOLES
4.76 (0.188) DIA.

6.35 (0.250) DIA.
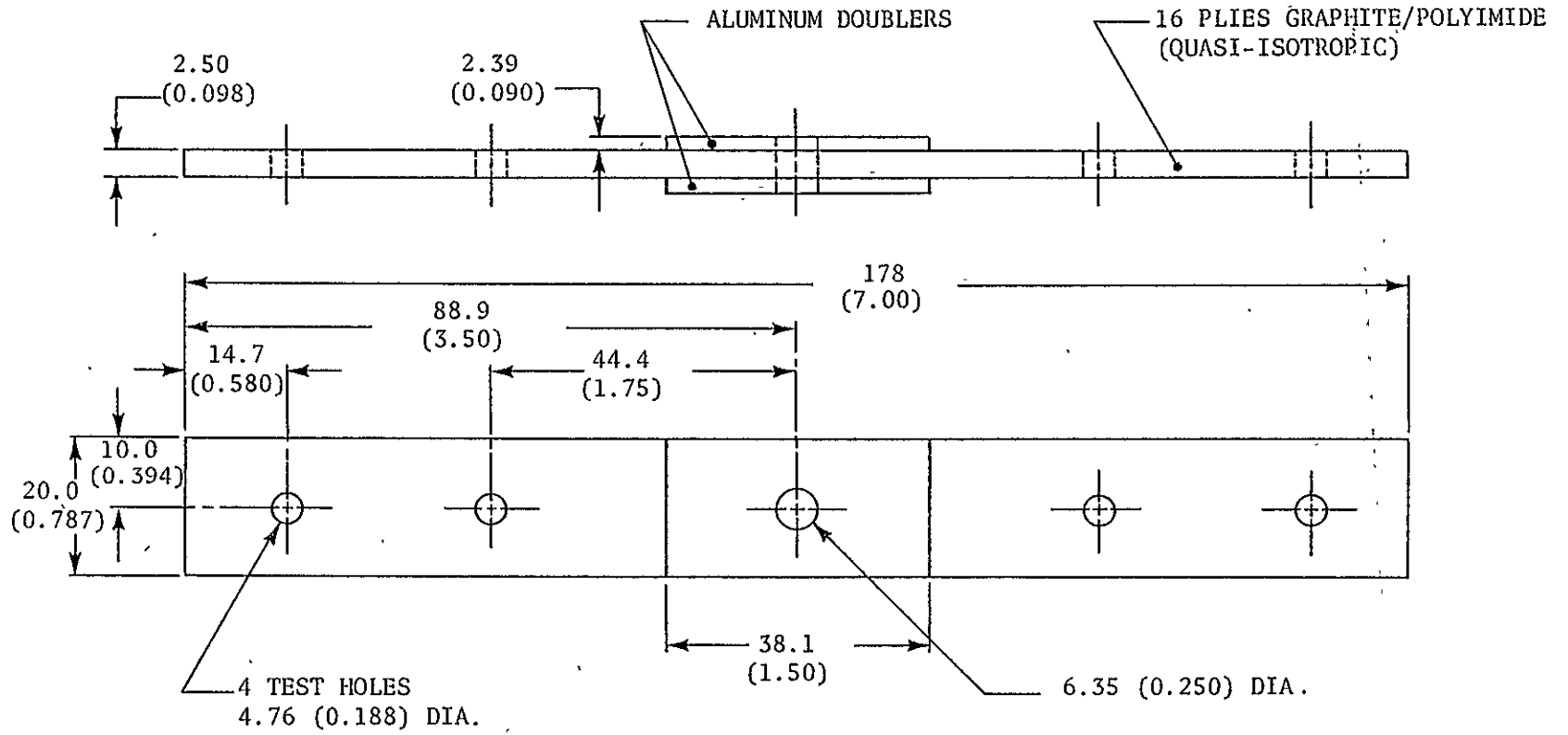
Figure 2. Specimen design for room temperature tests
[dimensions in mm (in.)].

STEEL LOAD
LINKS

6.35 (0.750)

15.88 (0.625)

15.88 (0.625)

6.35 (0.250)

GRAPHITE/
POLYIMIDE
TEST SPECIMEN

315.5°C	-156.7°C
TEST	TEST
TEMP.	TEMP.
311.7 °C	-156.7 °C
313.3	-156.7
314.4	-156.7
314.4	-156.7
315.0	-159.4
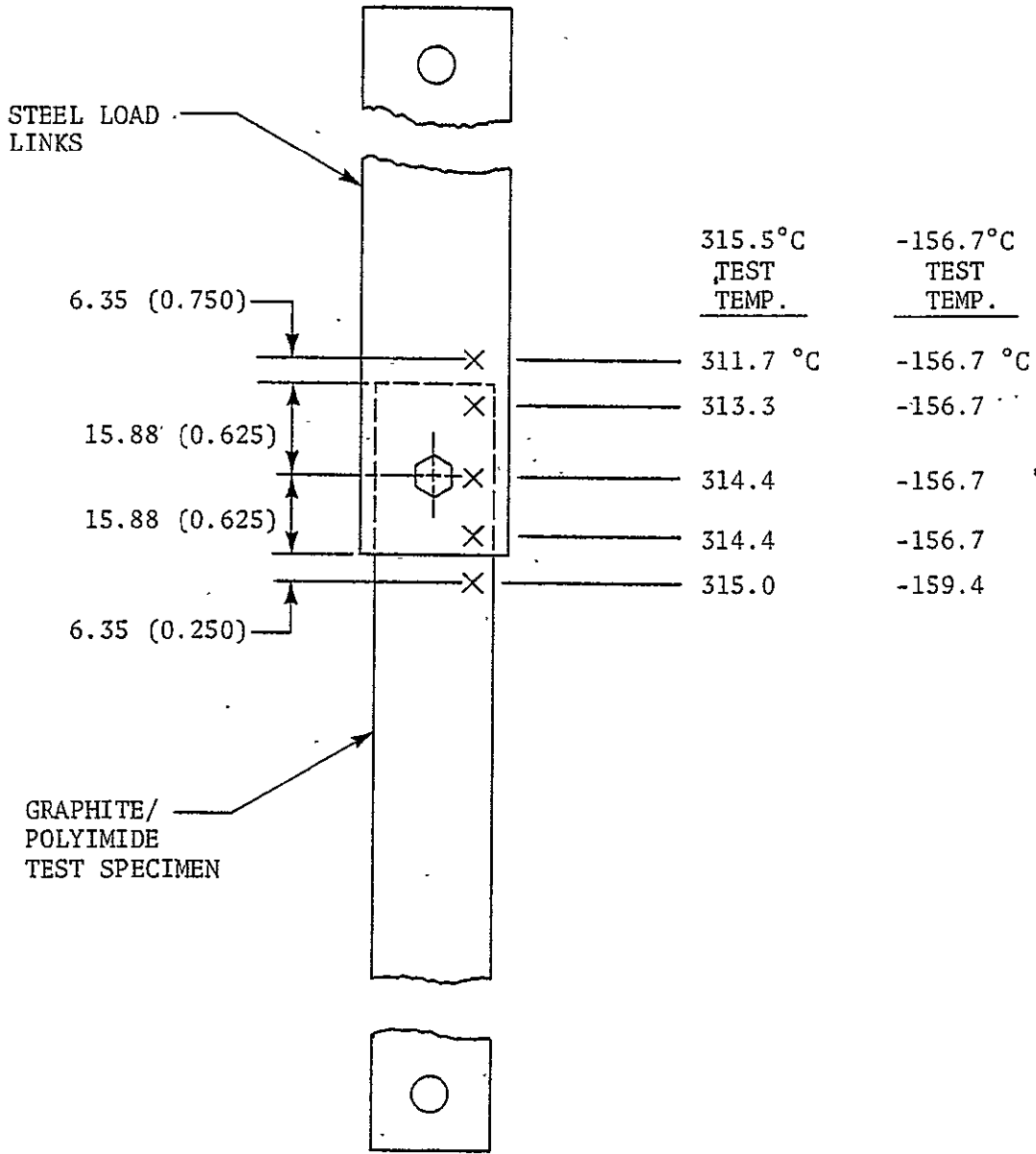
Figure 3. Temperature distribution on test specimen
[dimensions in mm (in.)].
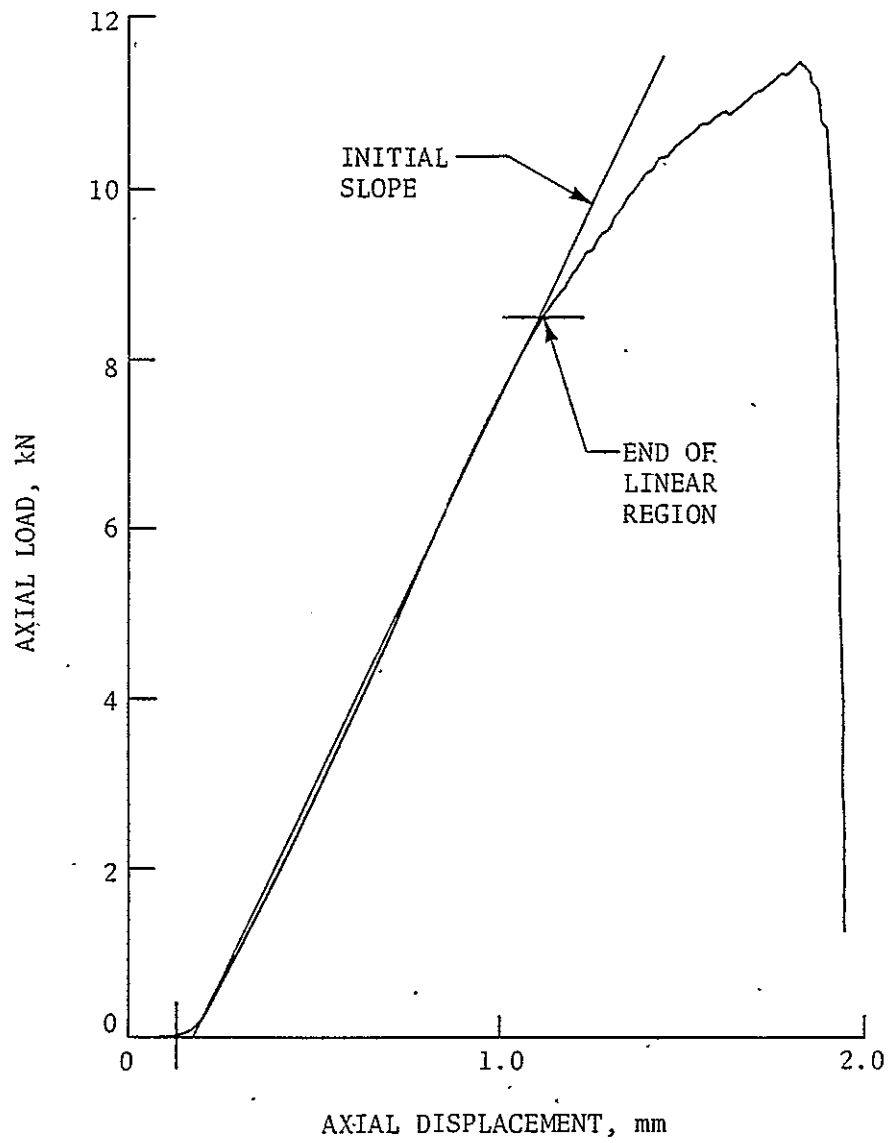
Figure 4. Load-deflection relation, net-section tension
failure.
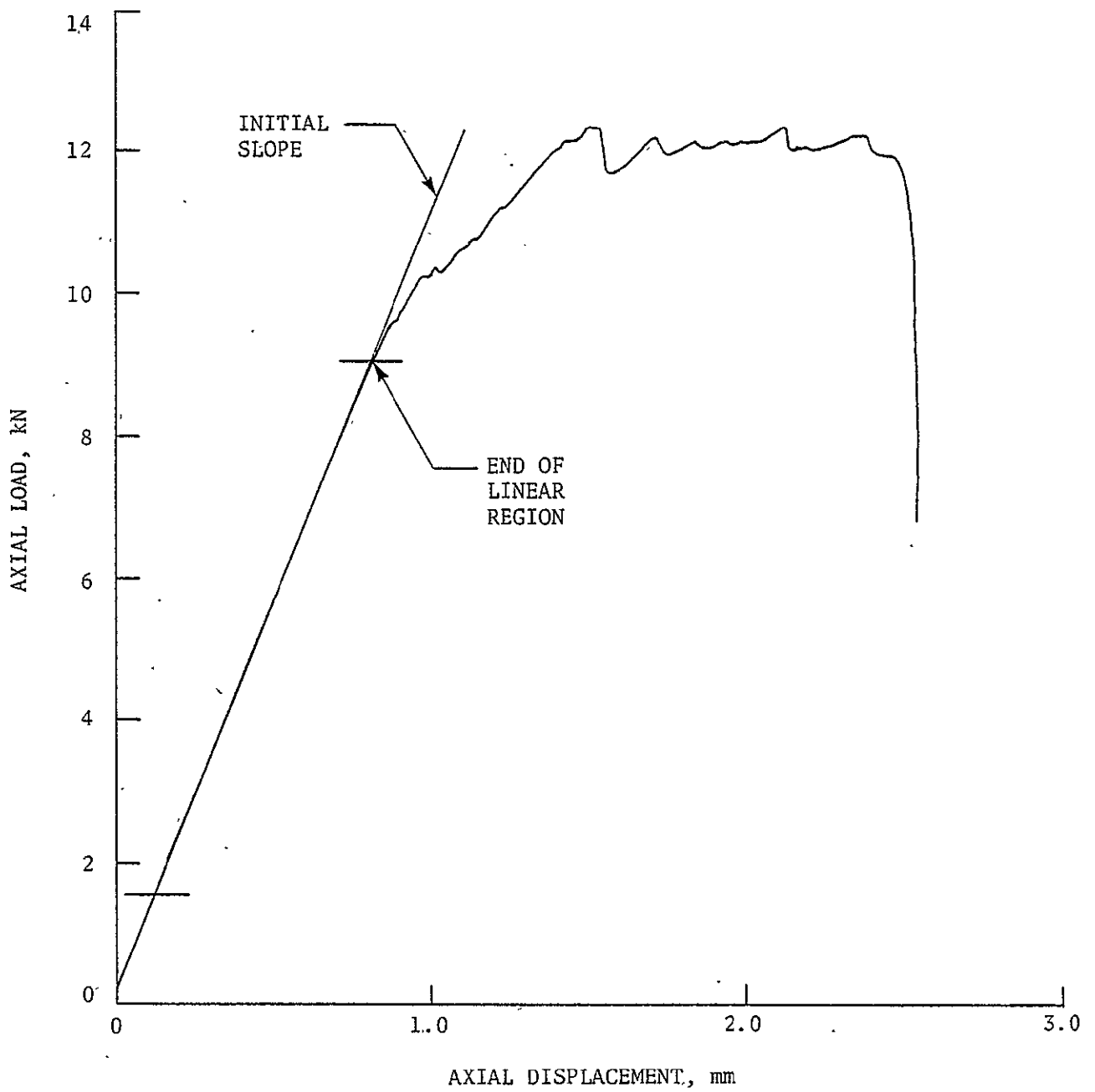
Figure 5.   Load-deflection relation, bearing failure.
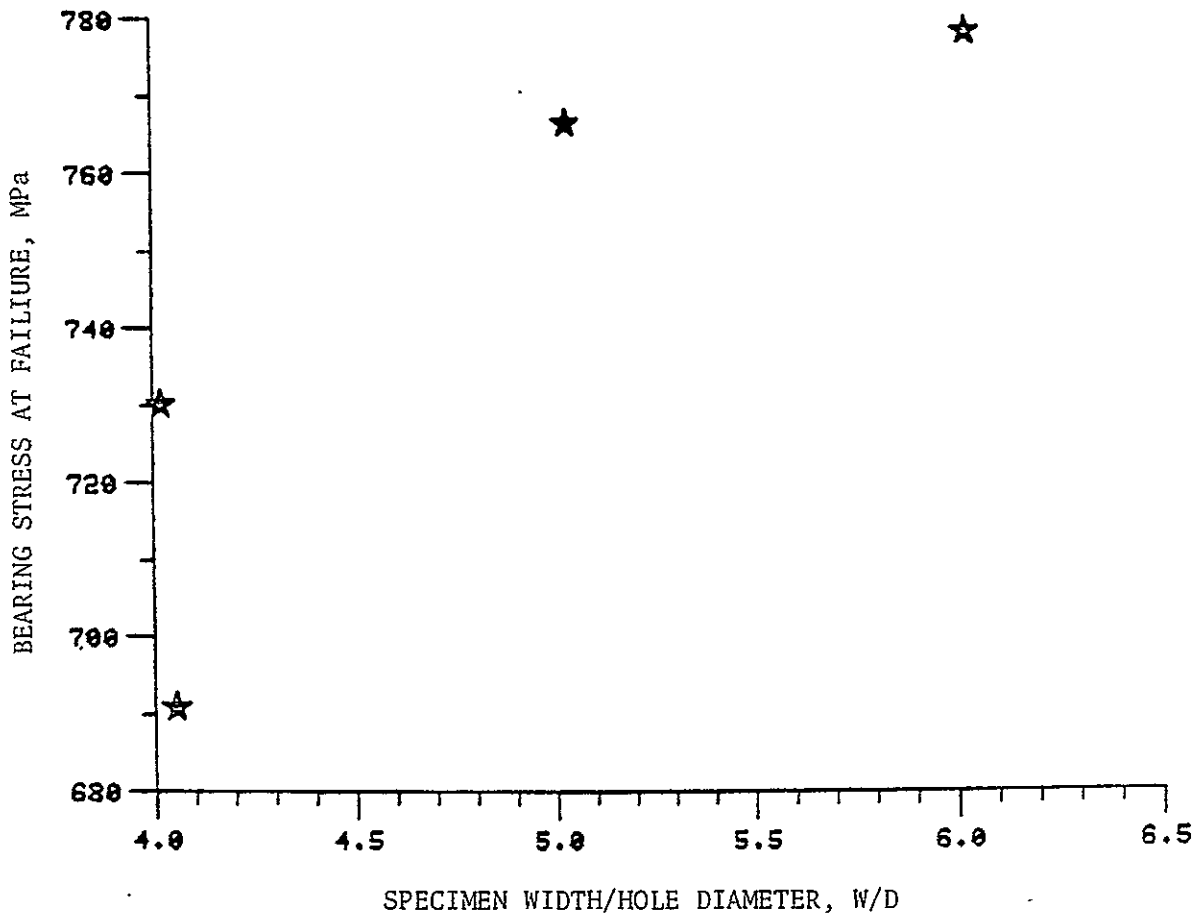
Figure 6. Bearing stress at failure vs. W/D, 315°C, raw data.
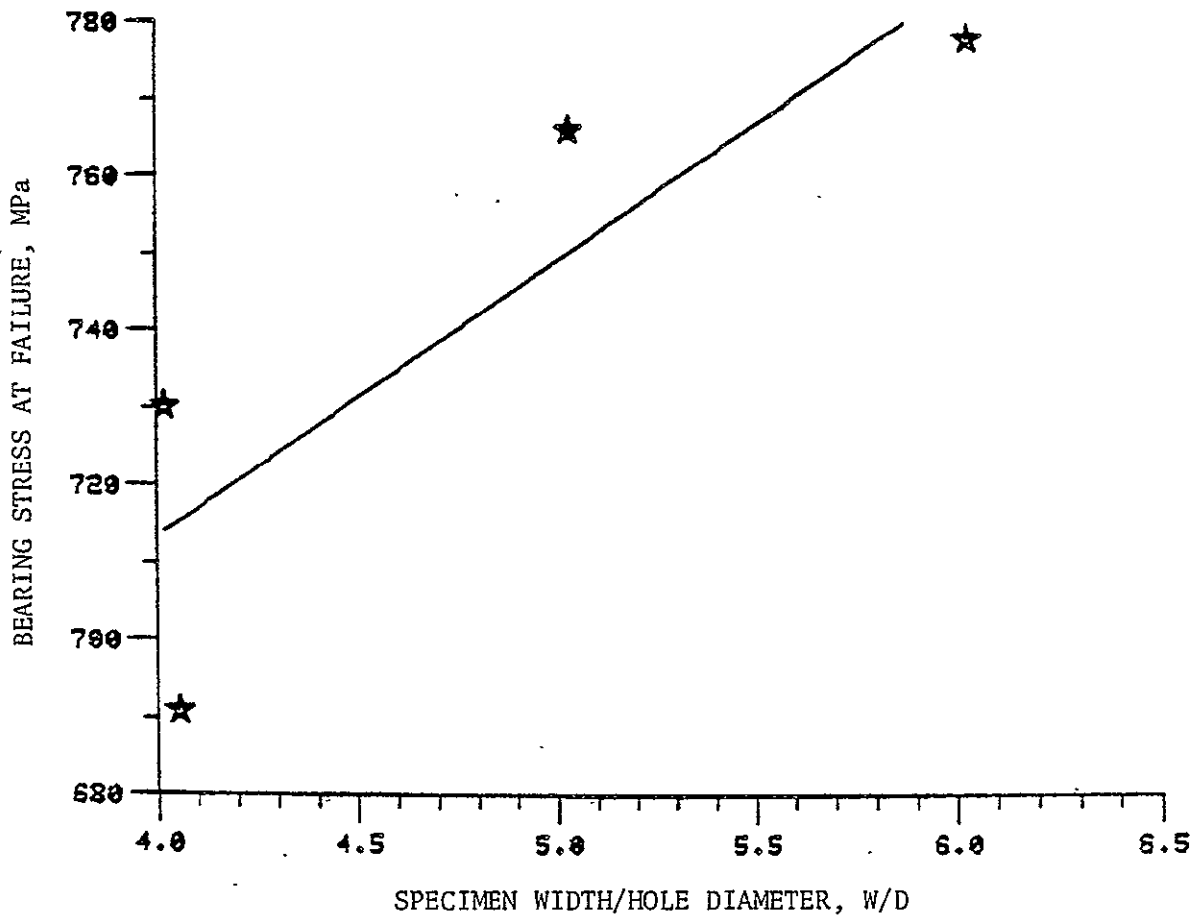
Figure 7. Bearing stress at failure vs. W/D, 315° C, first order curve.
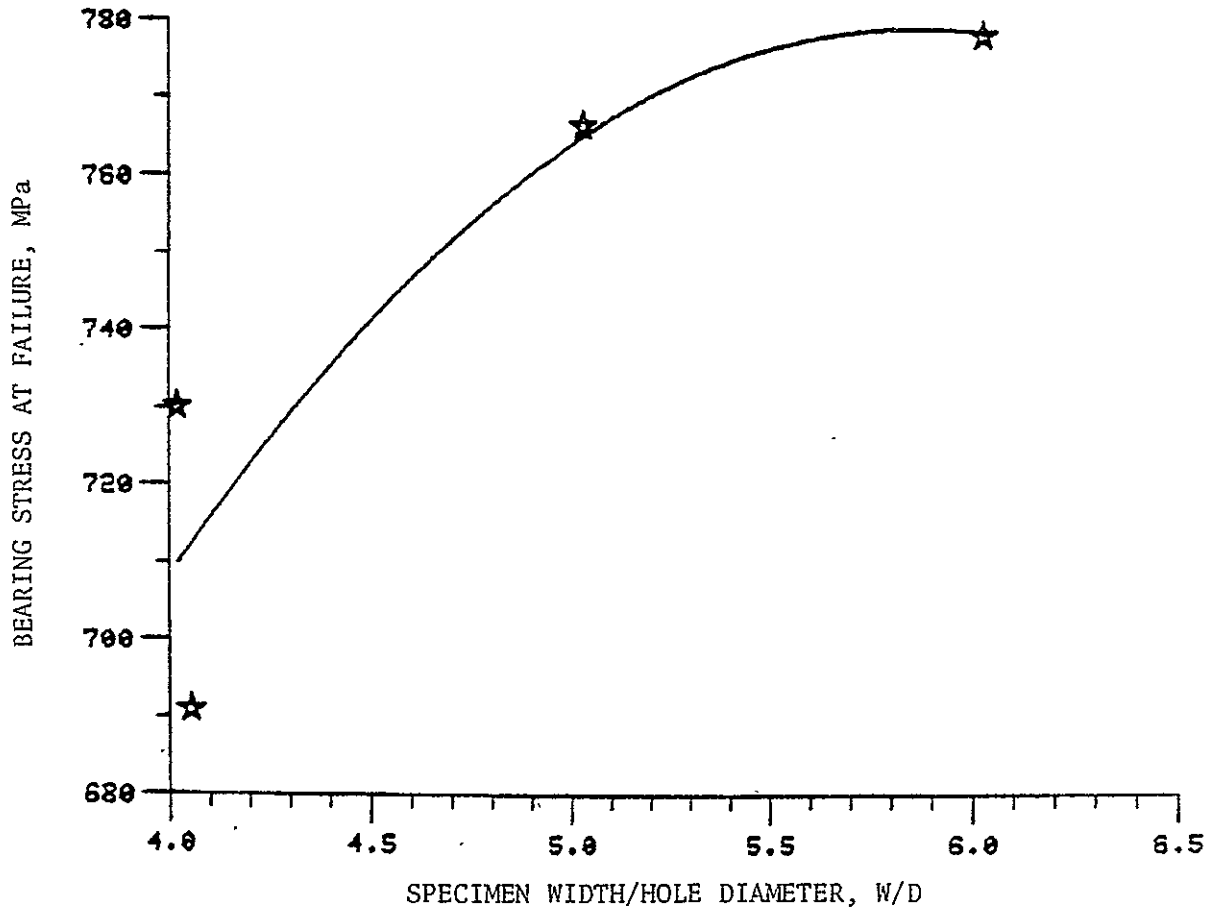
Figure 8. Bearing stress at failure vs. W/D, 315° C,
second order curve.
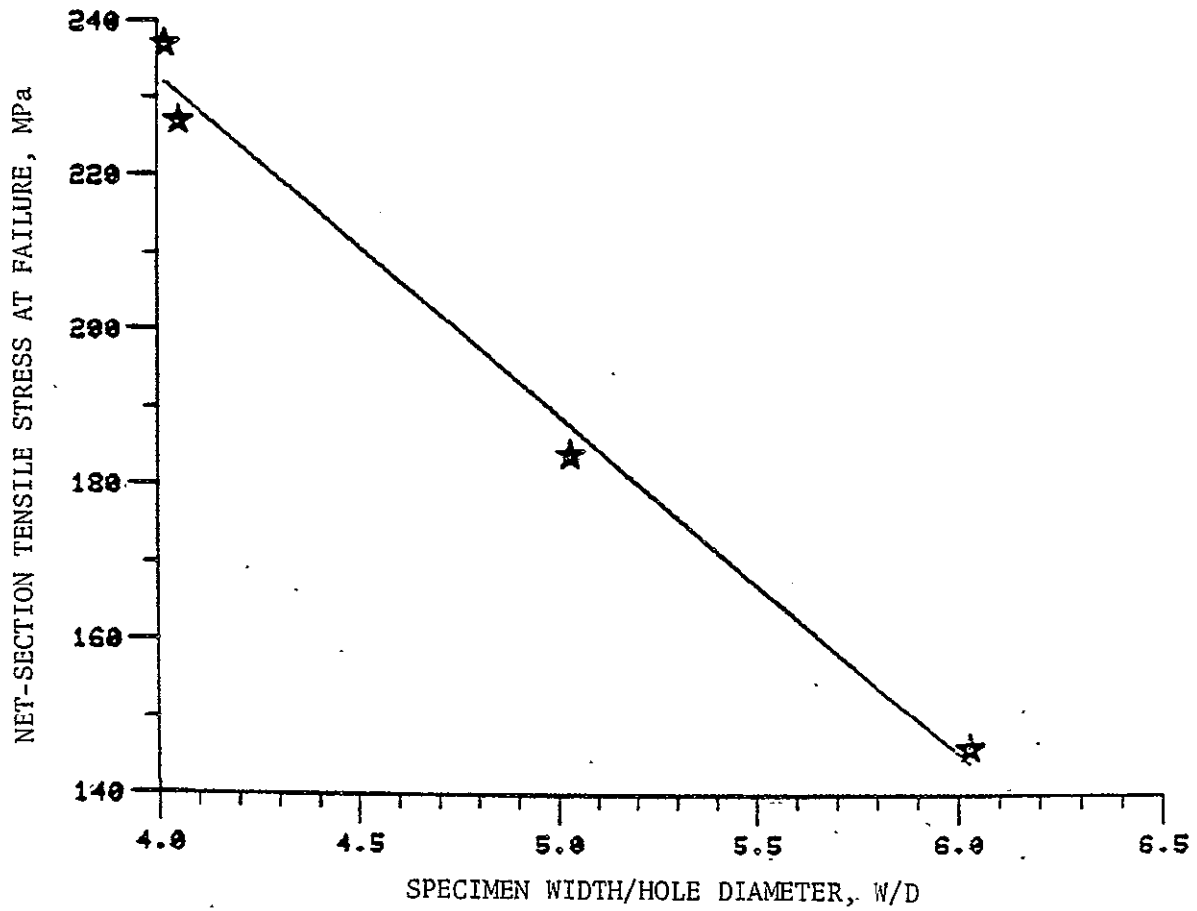
Figure 9. Net-section tensile stress at failure vs. W/D, 315° C, first order curve.
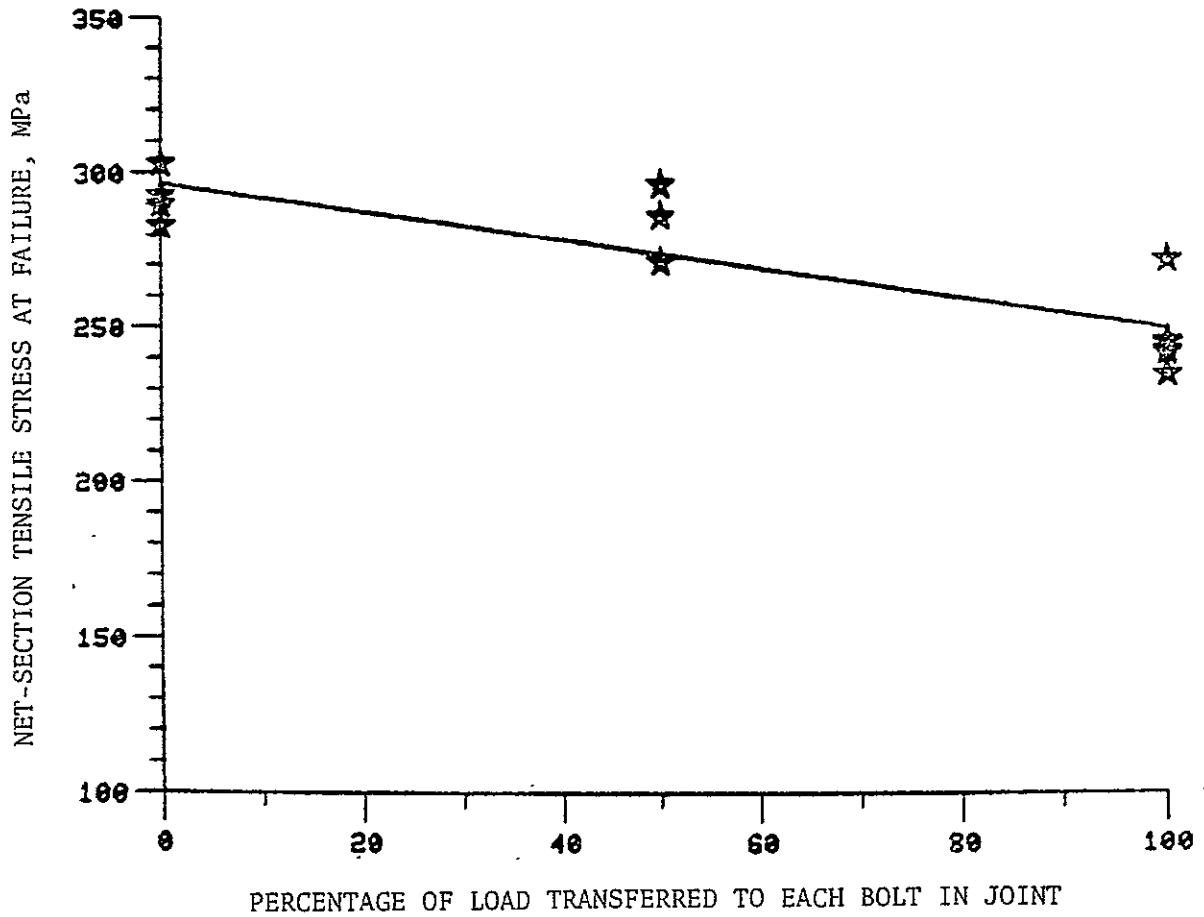
Figure 10. Effect of the number of bolts on load-carrying capacity, group A1, raw data.
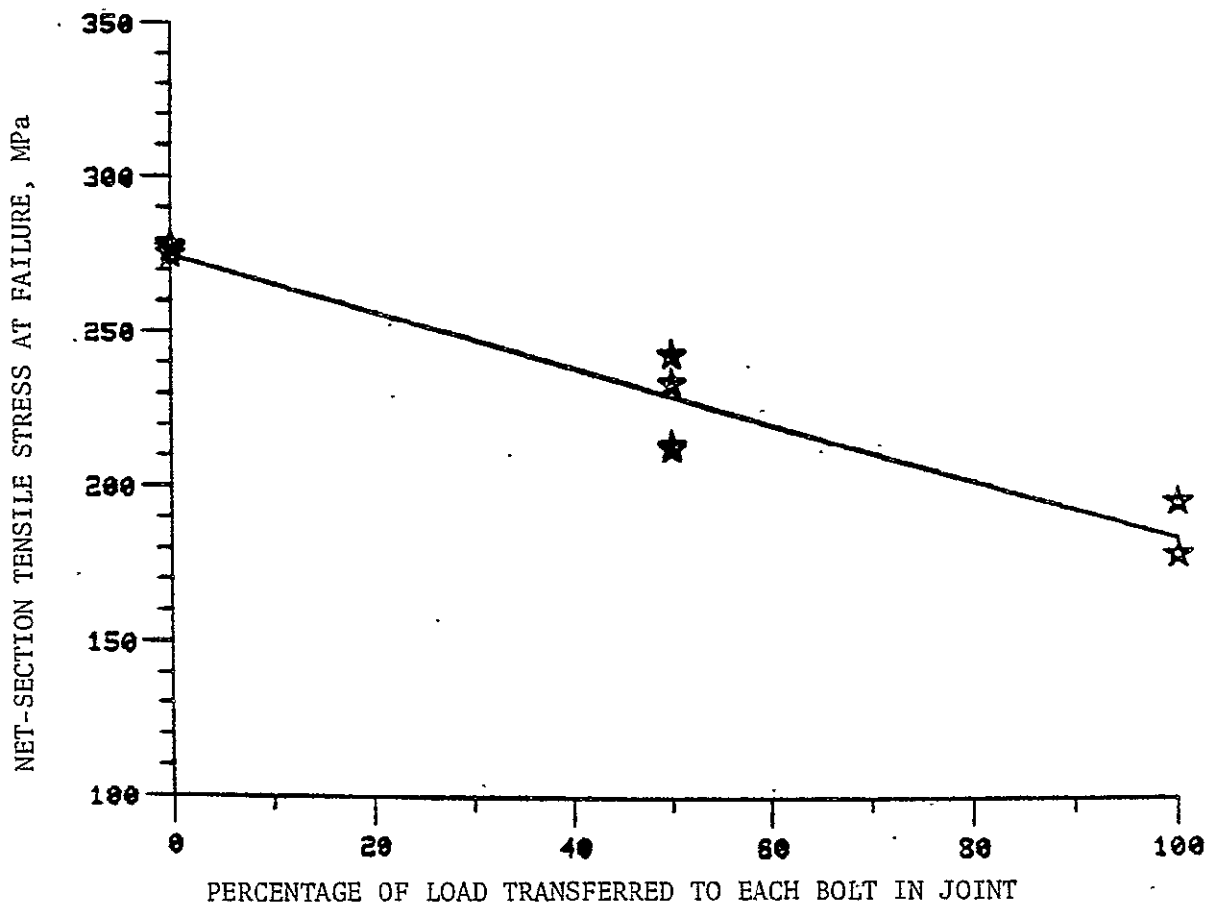
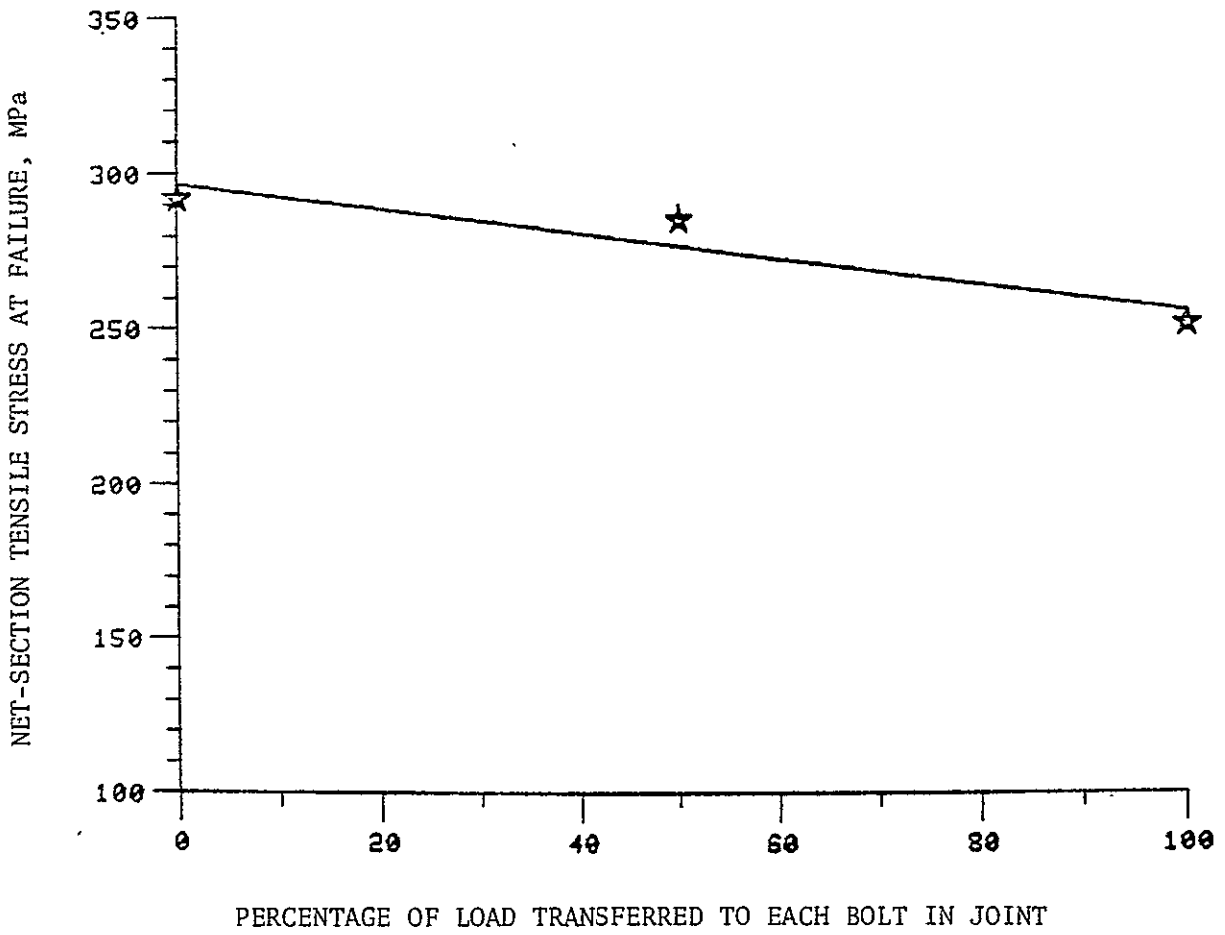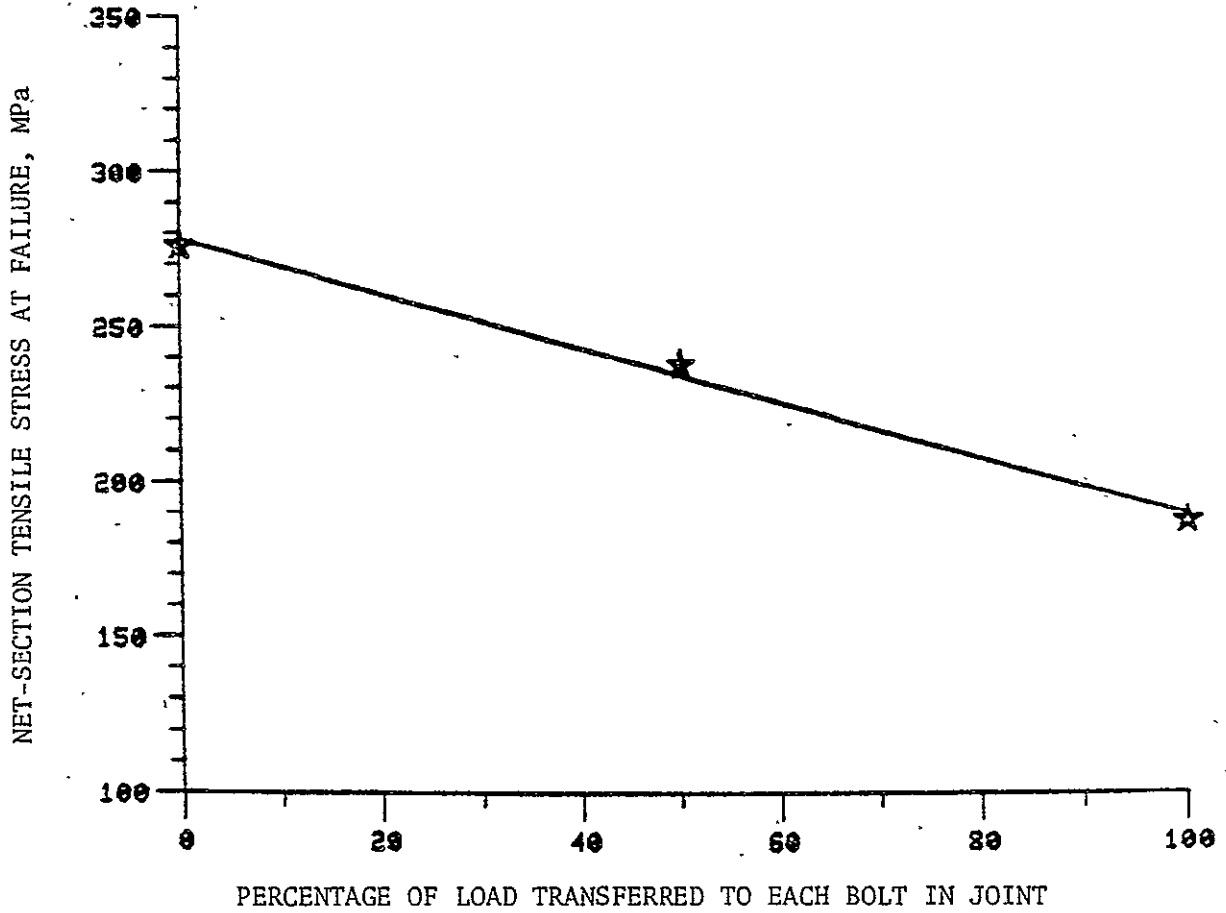Figure 11. Effect of the number of bolts on load-carrying capacity, group A2, raw data.
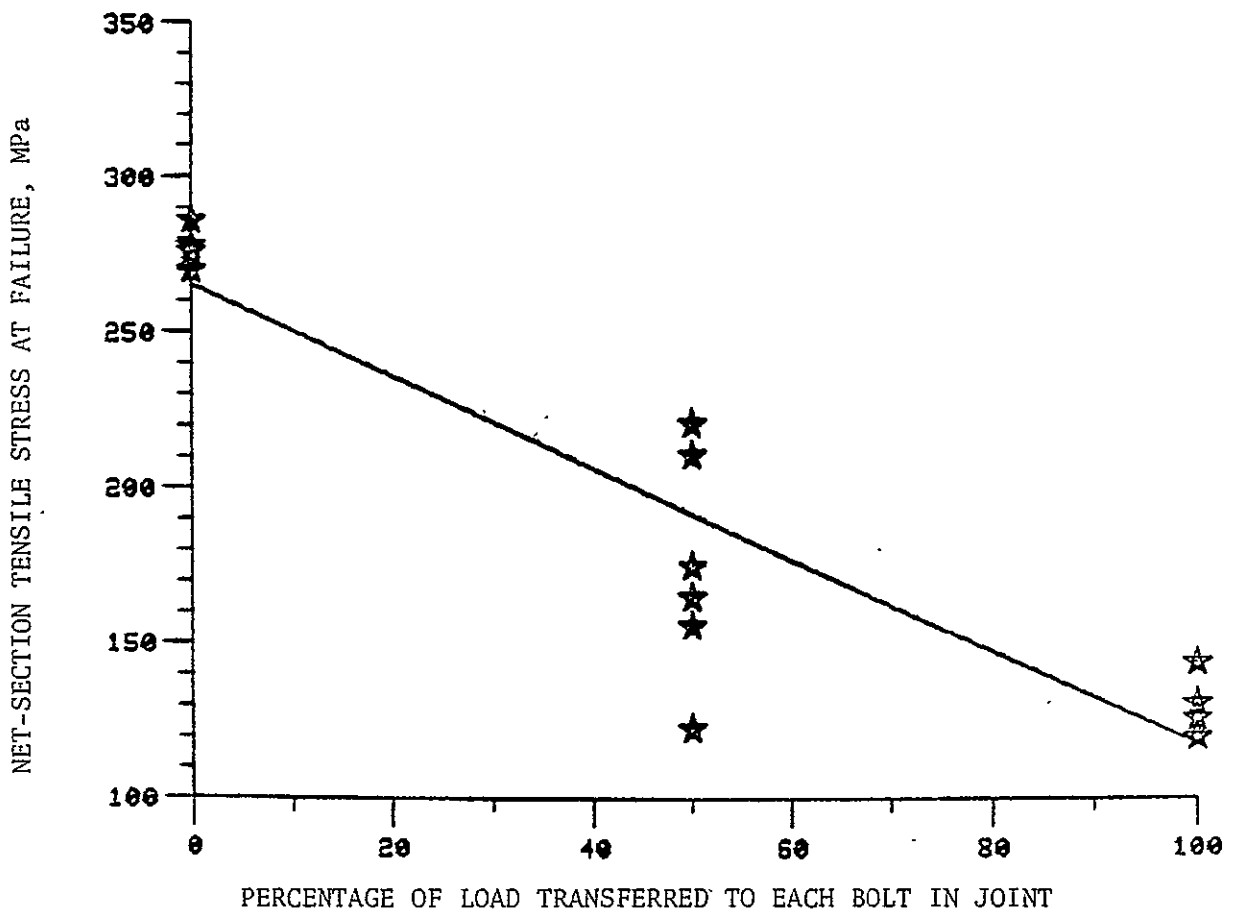
Figure 12. Effect of the number of bolts on load-carrying capacity, group A3, raw data.
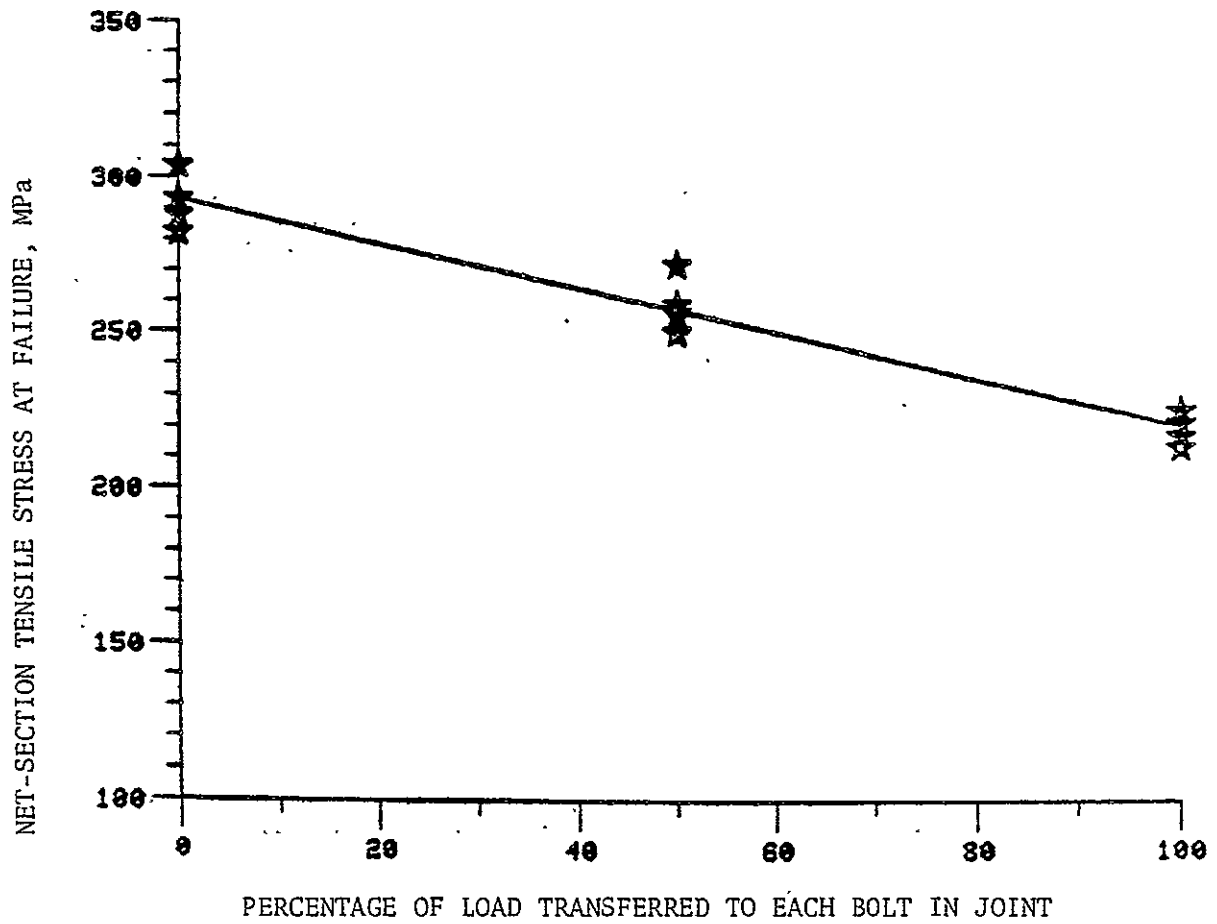
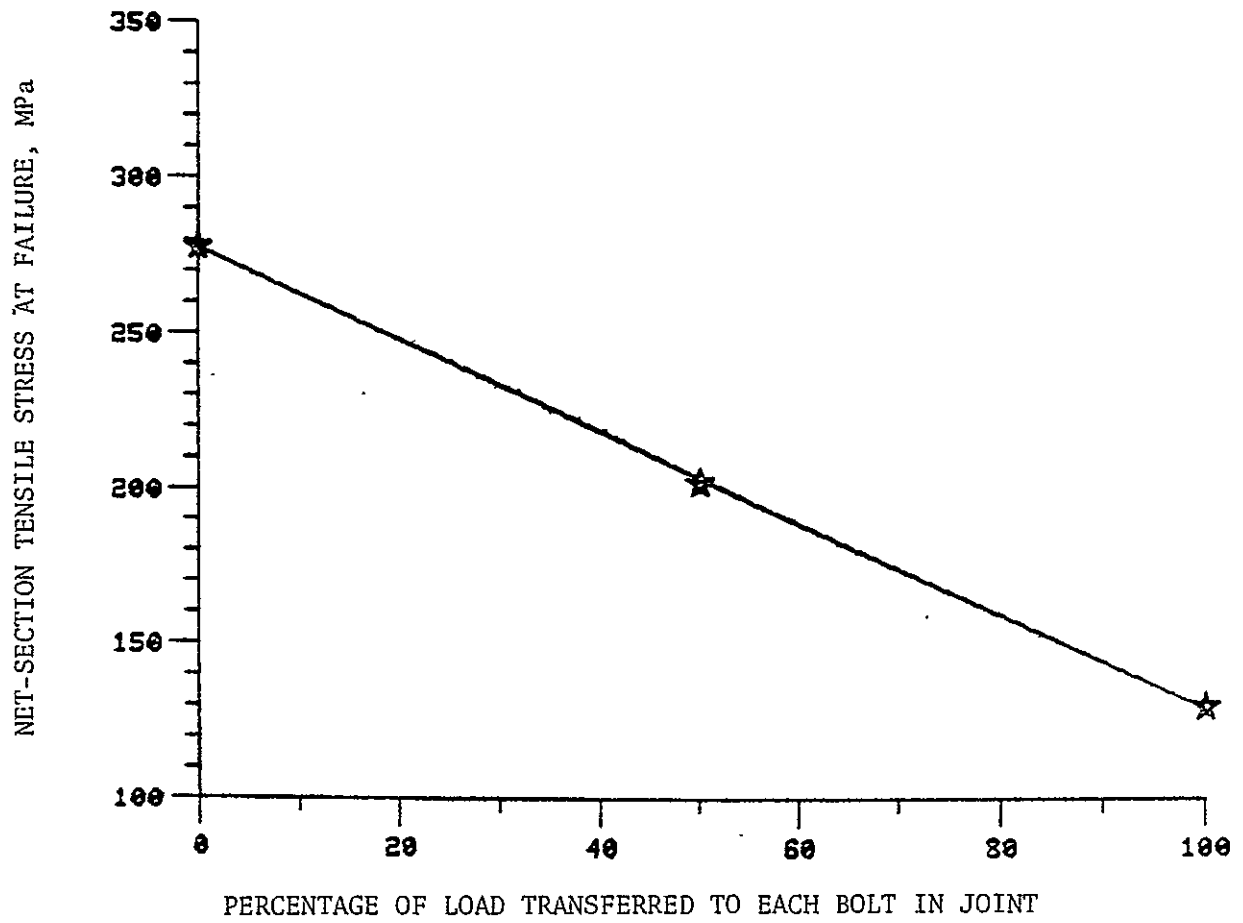Figure 13. Effect of the number of bolts on load-carrying capacity, group A4, raw data.
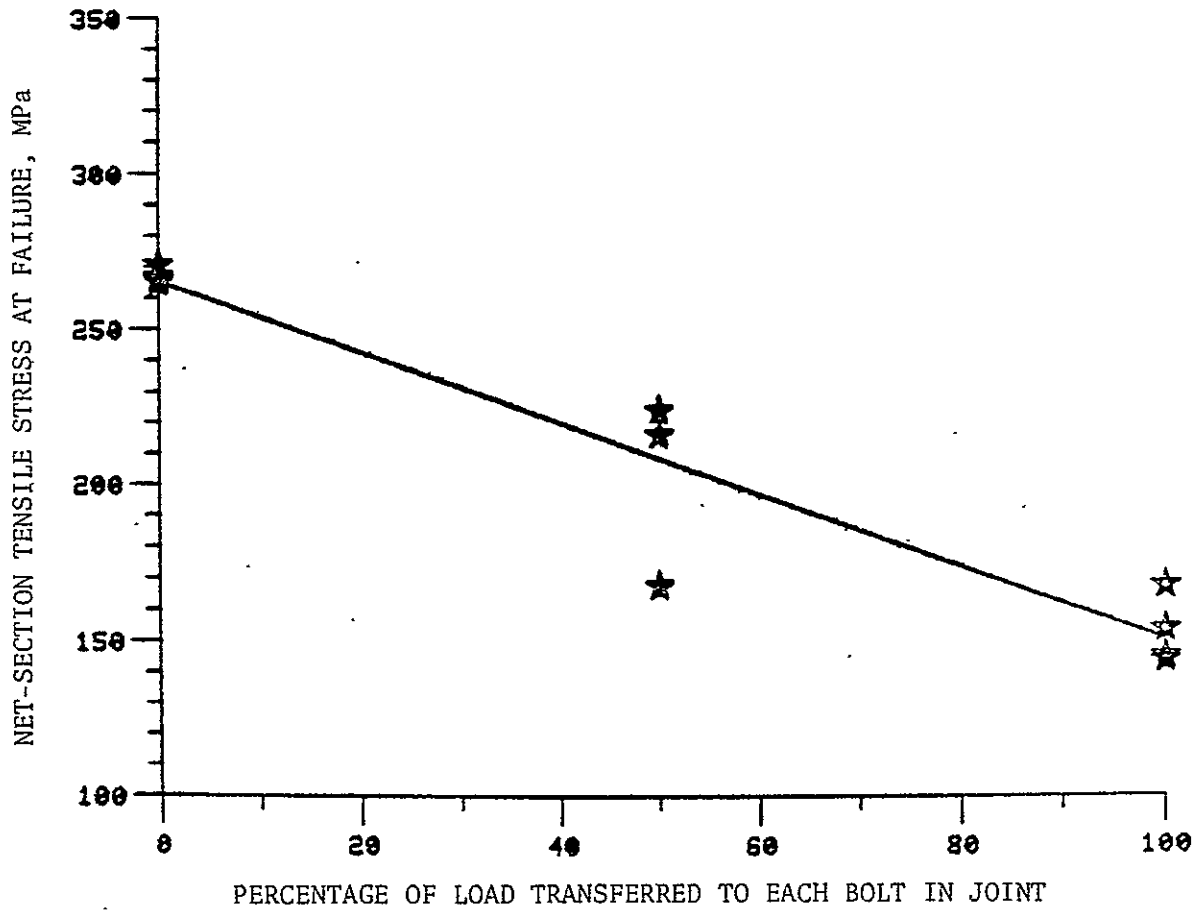
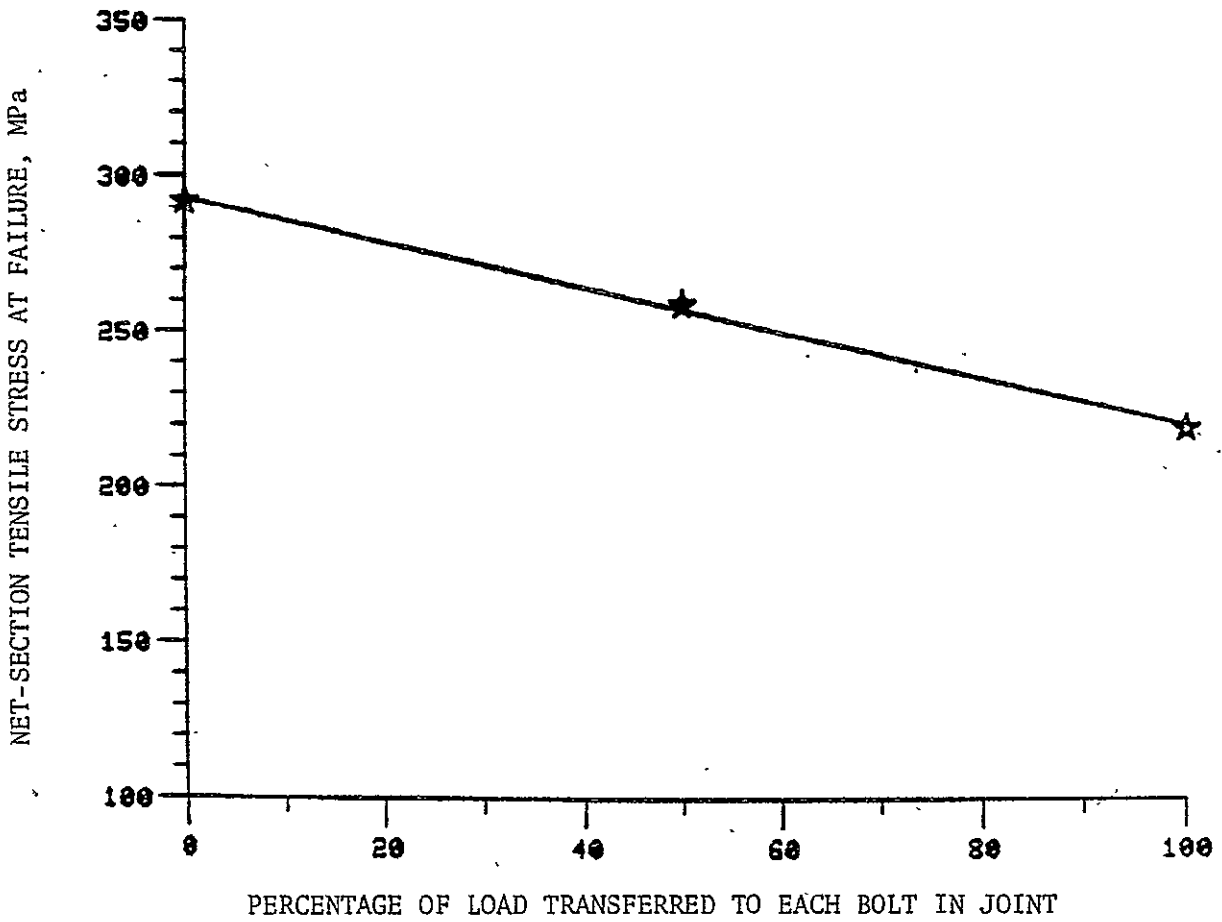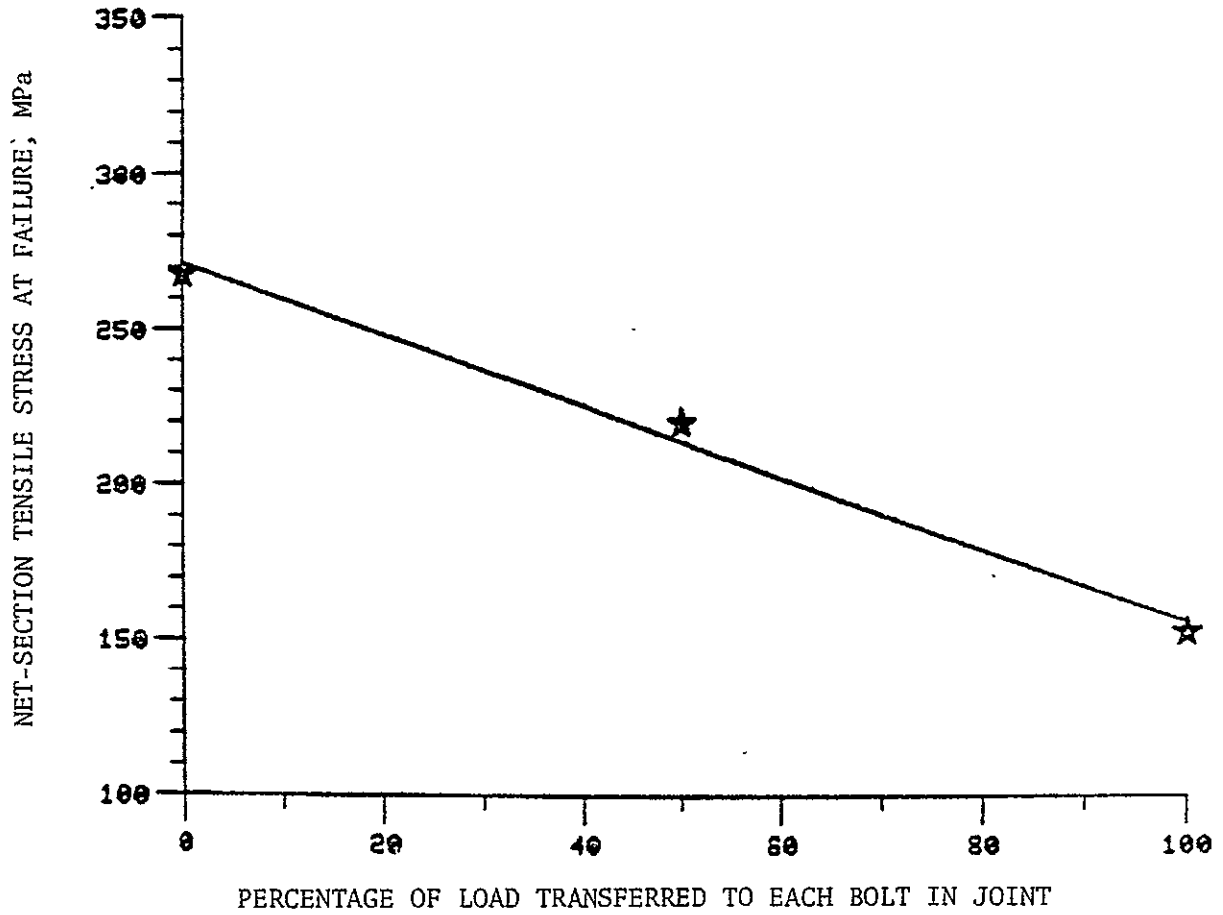Figure 14. Effect of the number of bolts on load-carrying capacity, group A5, raw data.
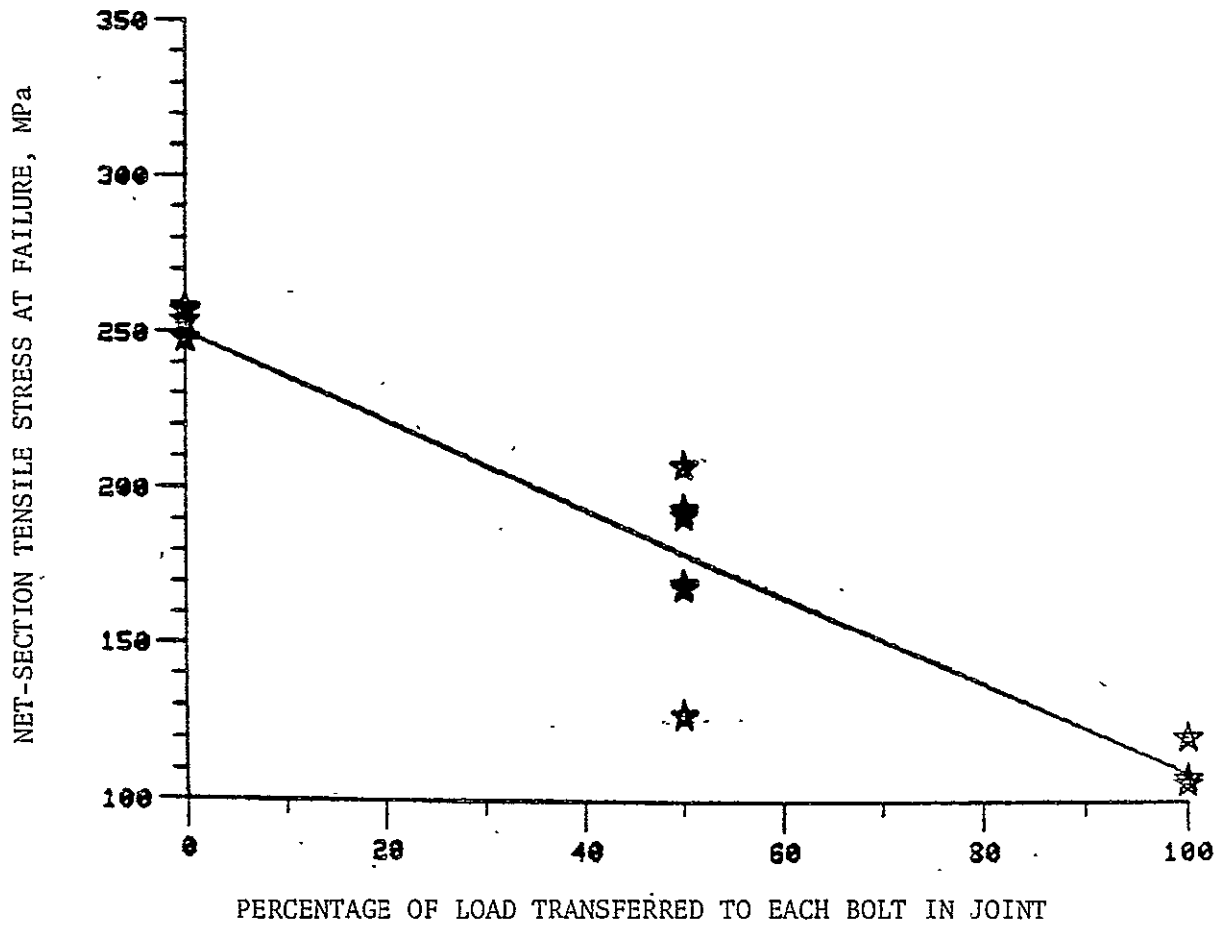
Figure 15. Effect of the number of bolts on load-carrying capacity, group A6, raw data.
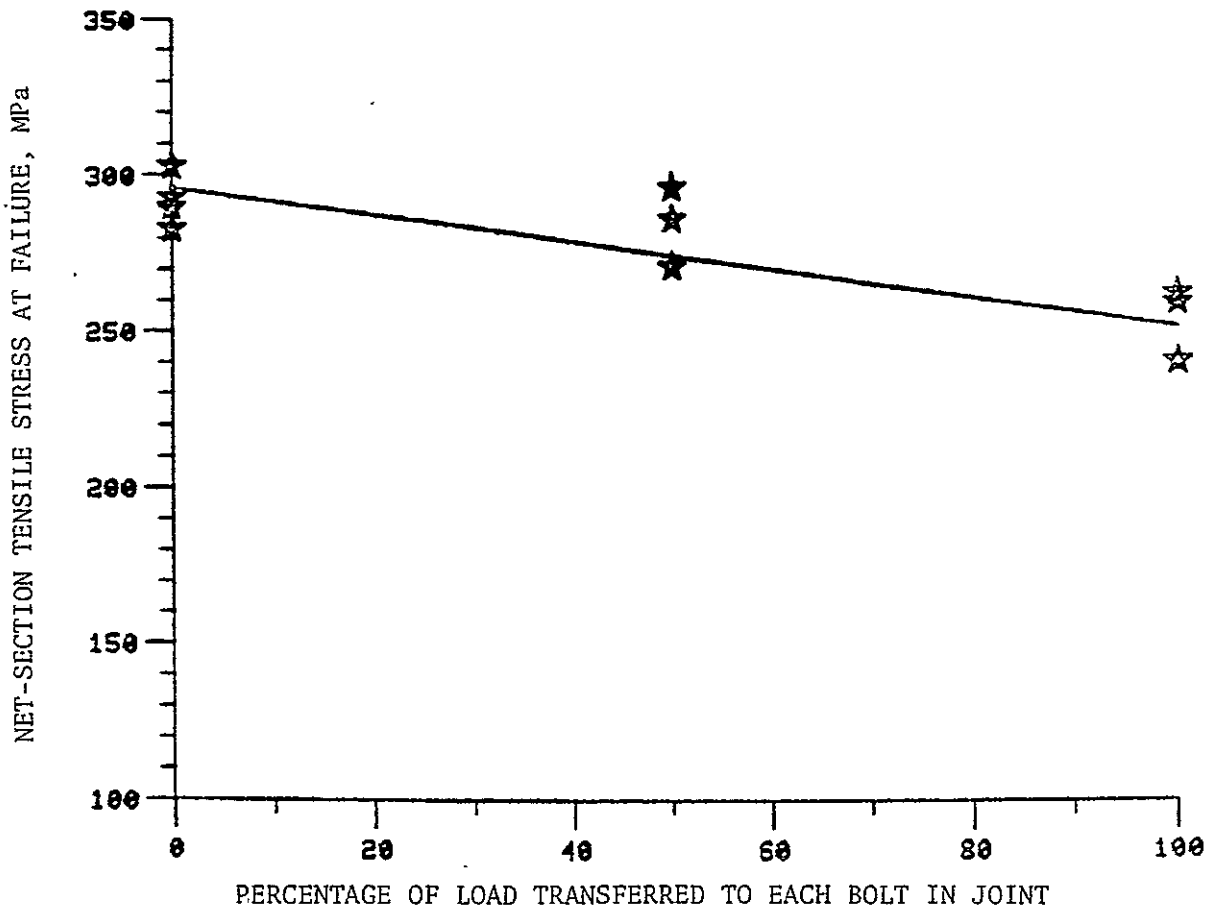
Figure 16. Effect of the number of bolts on load-carrying capacity,
group B1, raw data.
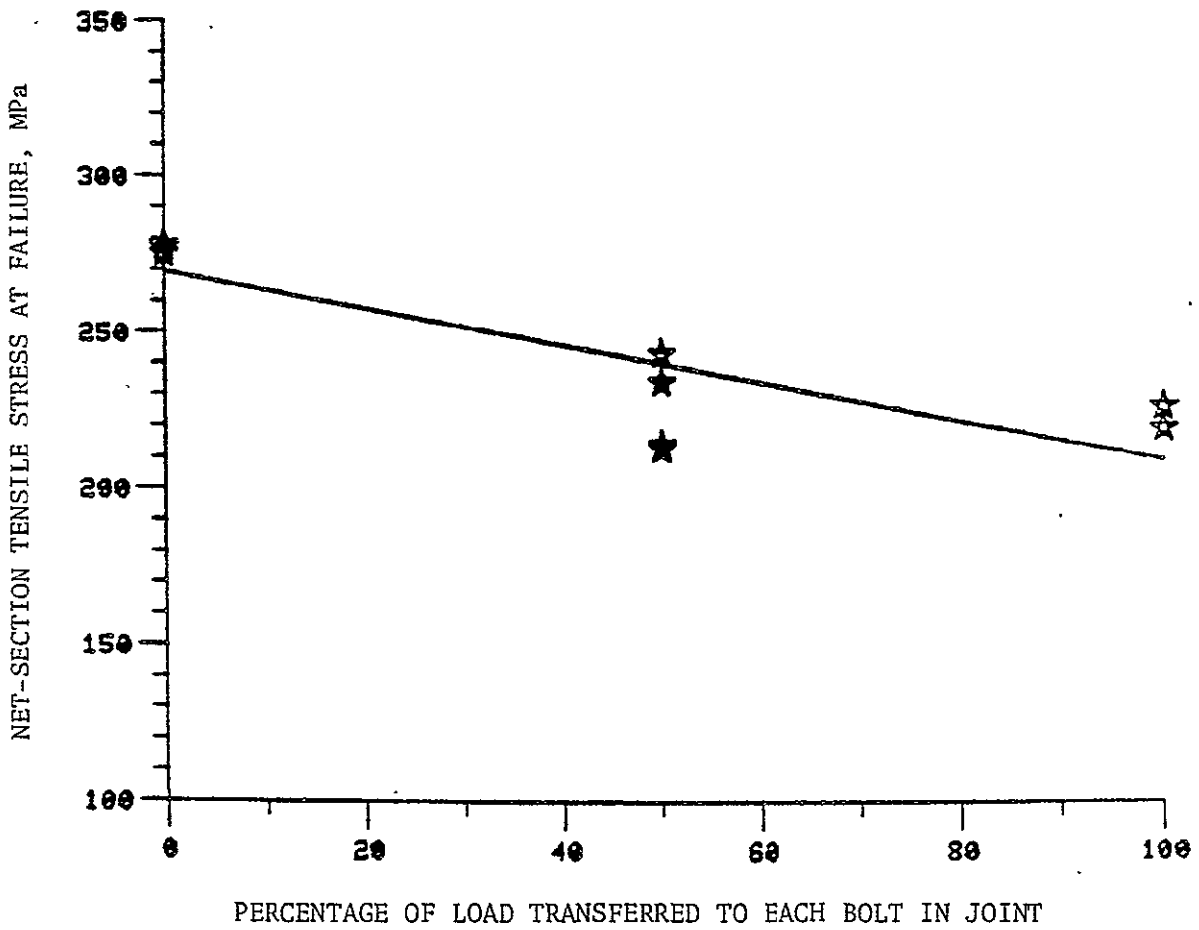
Figure 17.   Effect of the number of bolts on load-carrying capacity,
group B2, raw data.
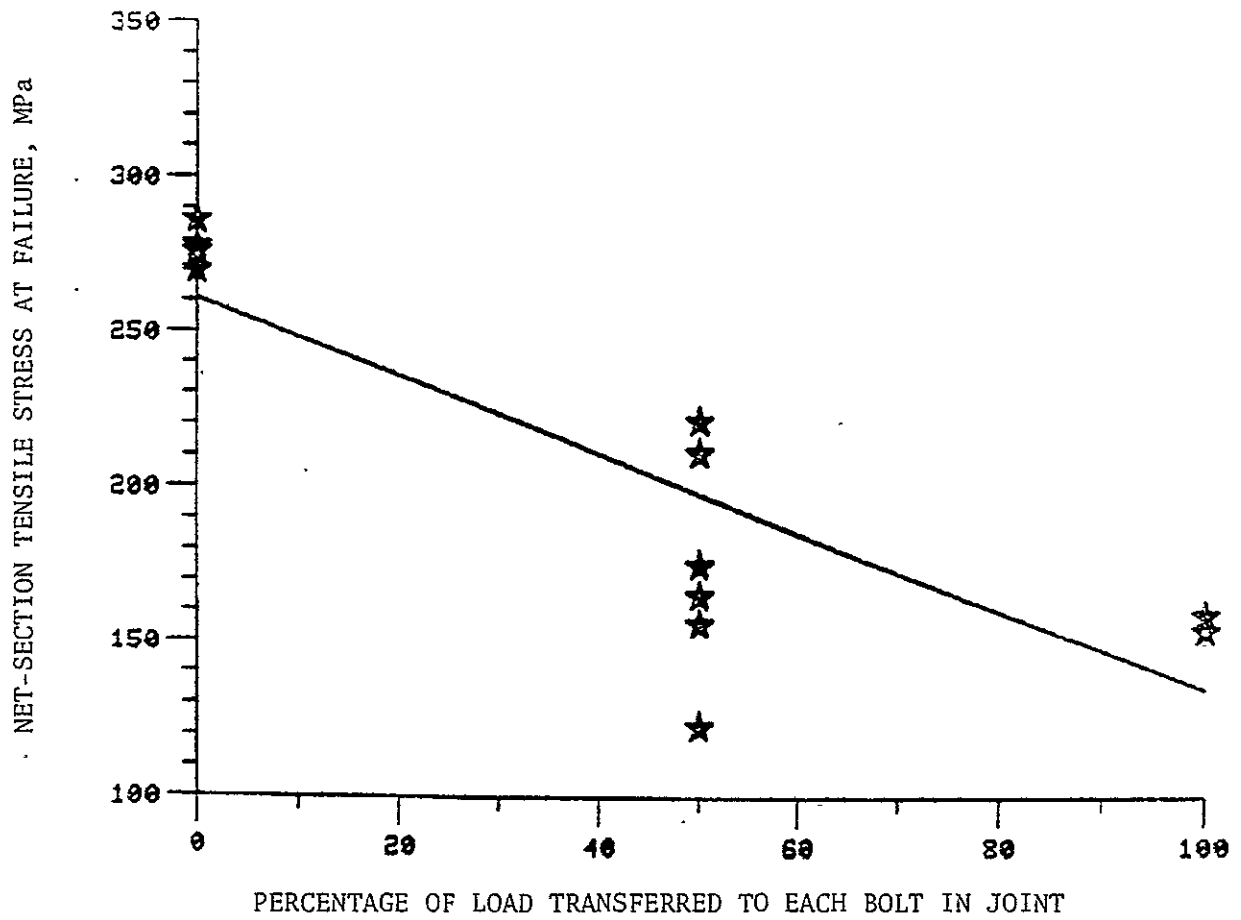
Figure 18. Effect of the number of bolts on load-carrying capacity, group B3, raw data.
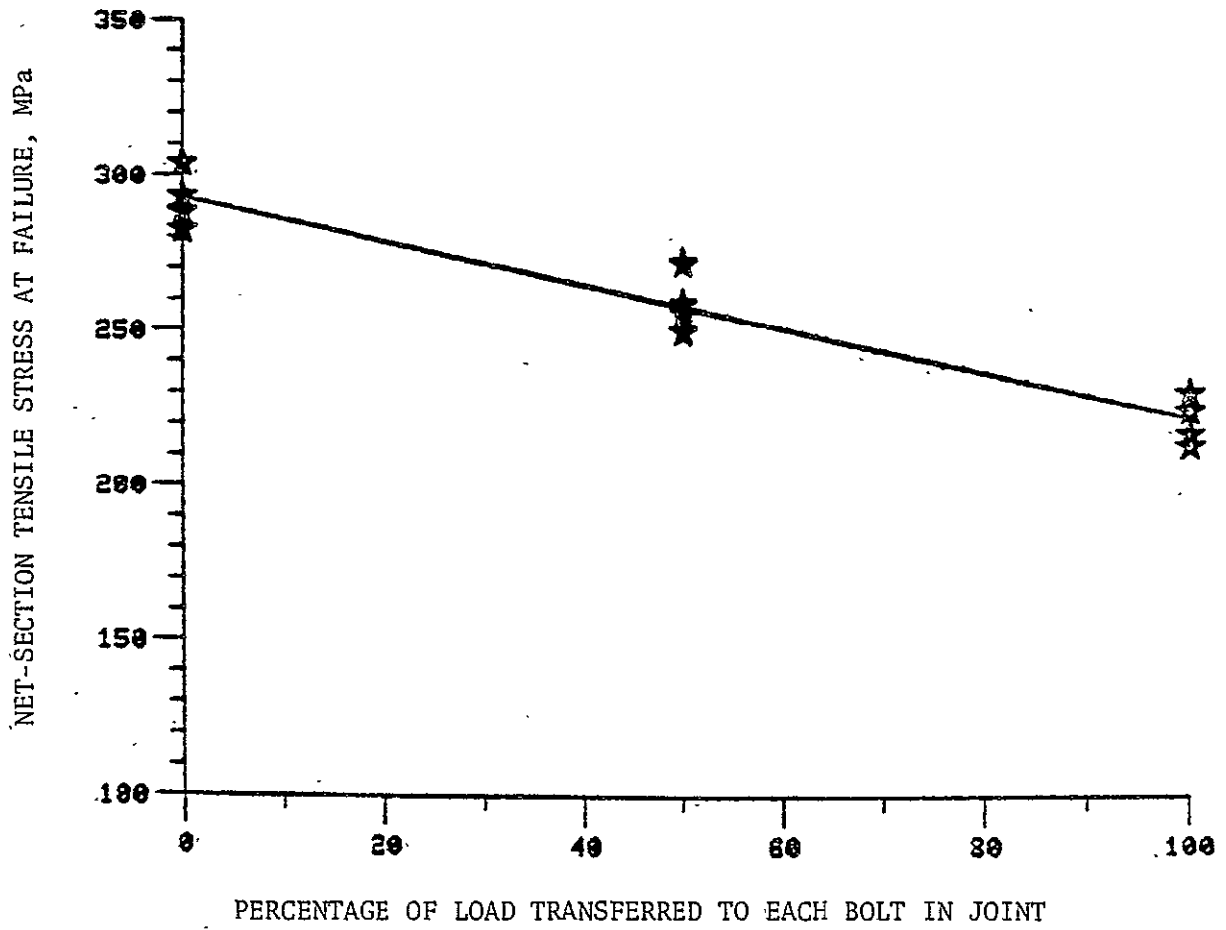
Figure 19. Effect of the number of bolts on load-carrying capacity,
group B4, raw data.
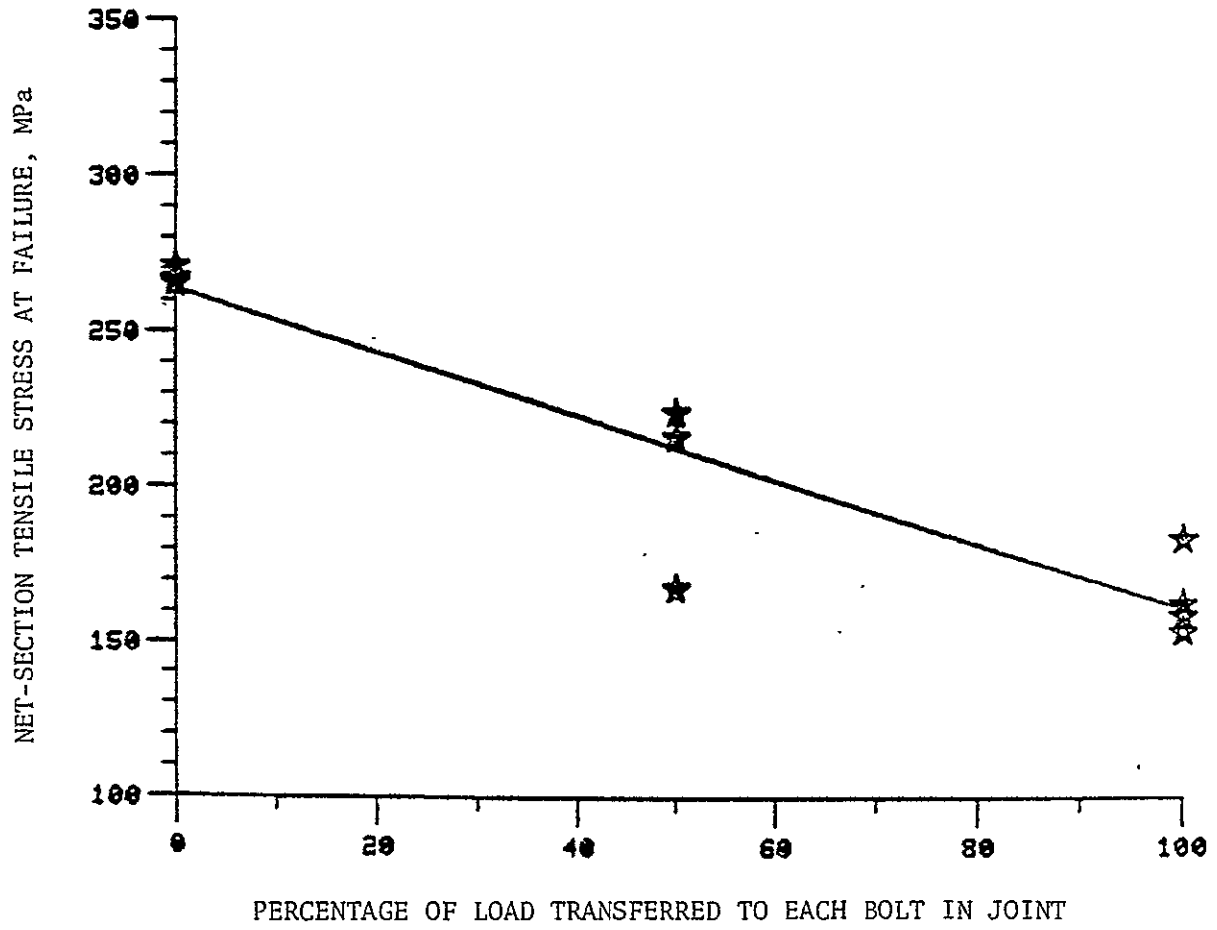
Figure 20. Effect of the number of bolts on load-carrying capacity, group B5, raw data.
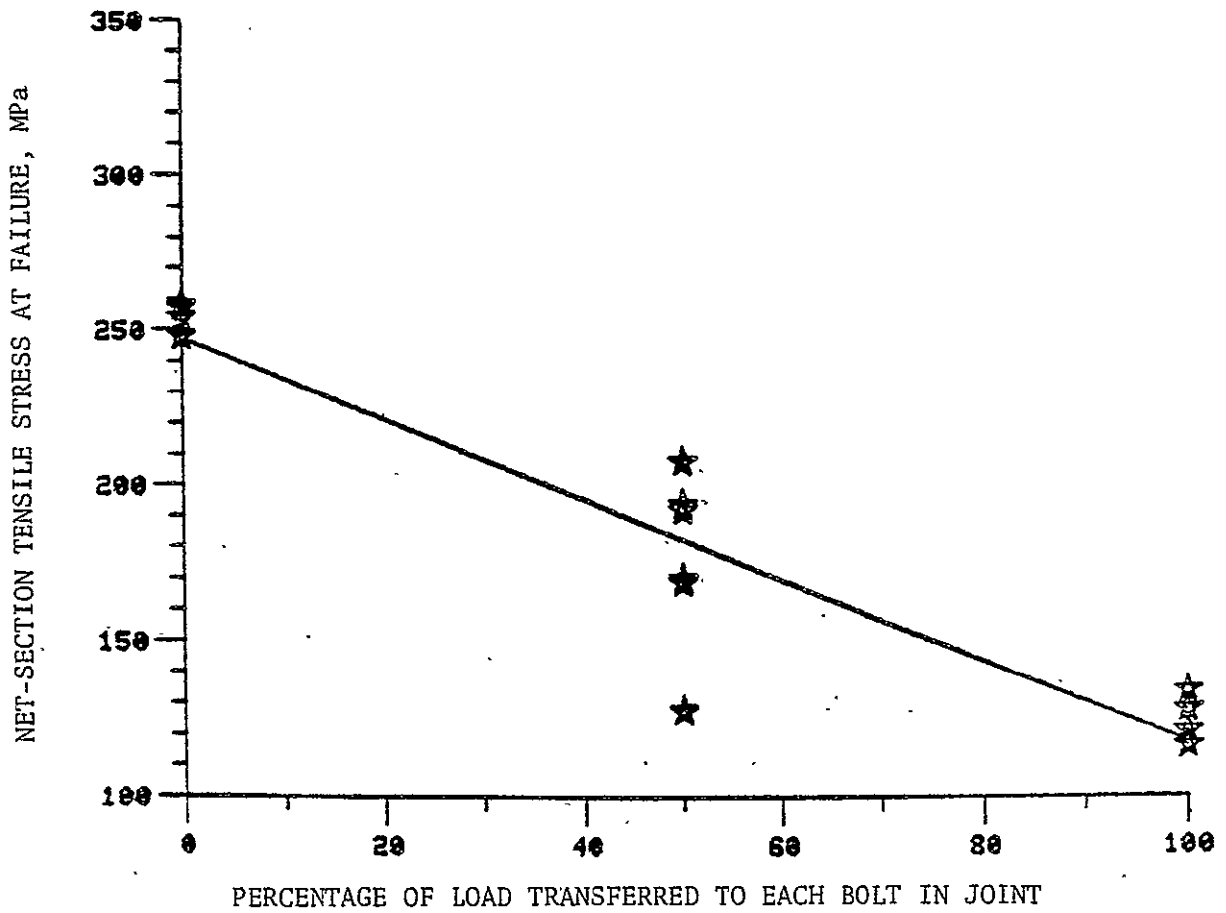
Figure 21. Effect of the number of bolts on load-carrying capacity, group B6, raw data.
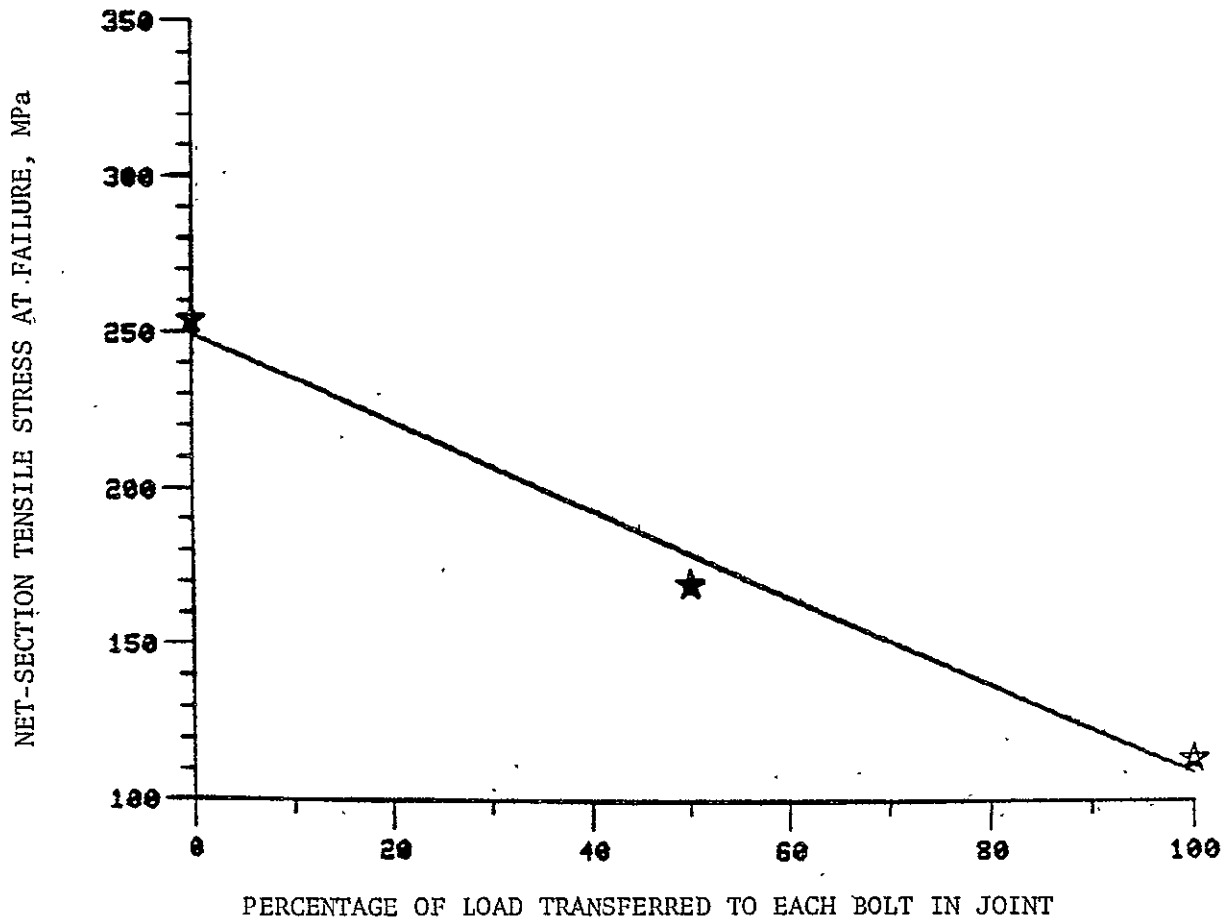
Figure 22. Effect of the number of bolts on load-carrying capacity, group Al, averaged data.

Figure 23. Effect of the number of bolts on load-carrying capacity, group A2, averaged data.
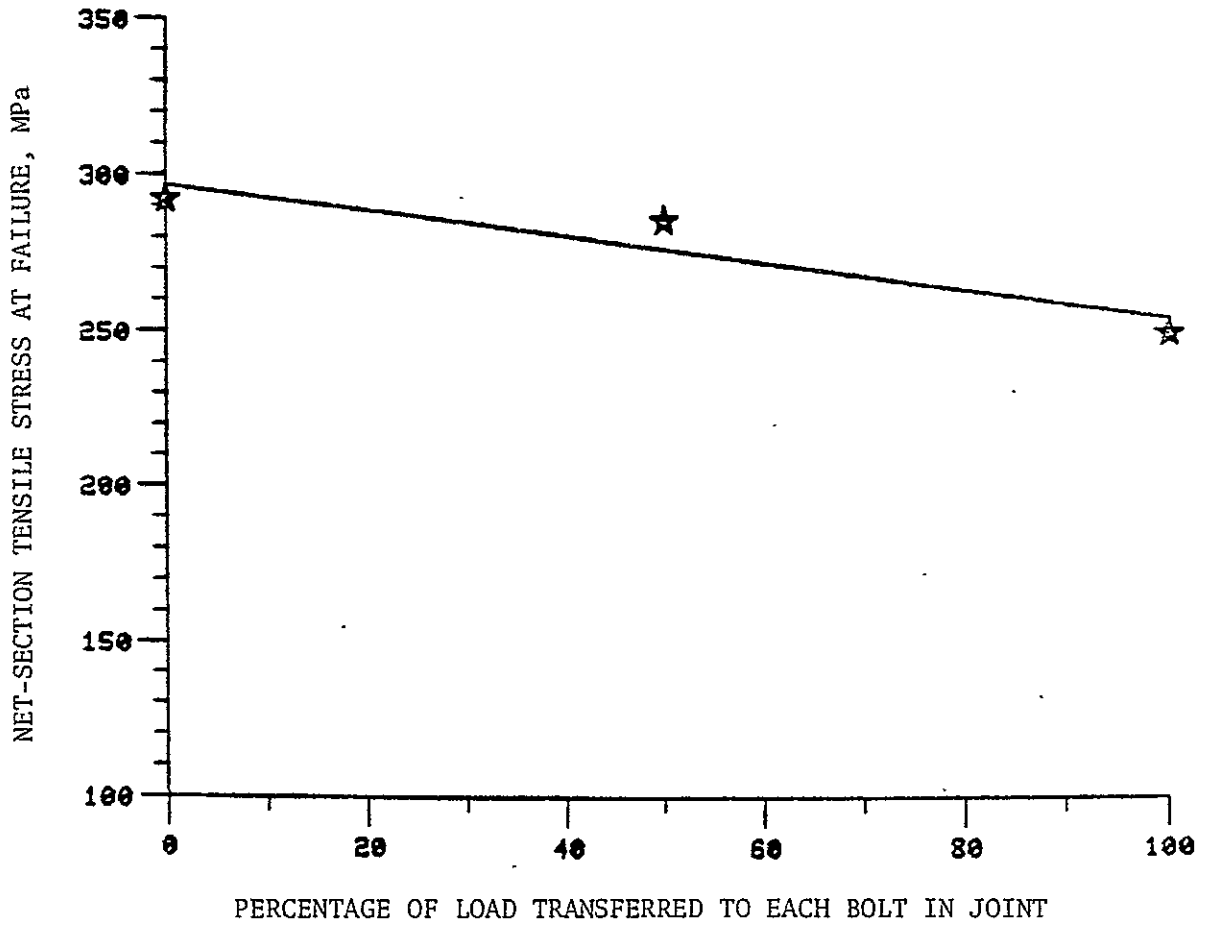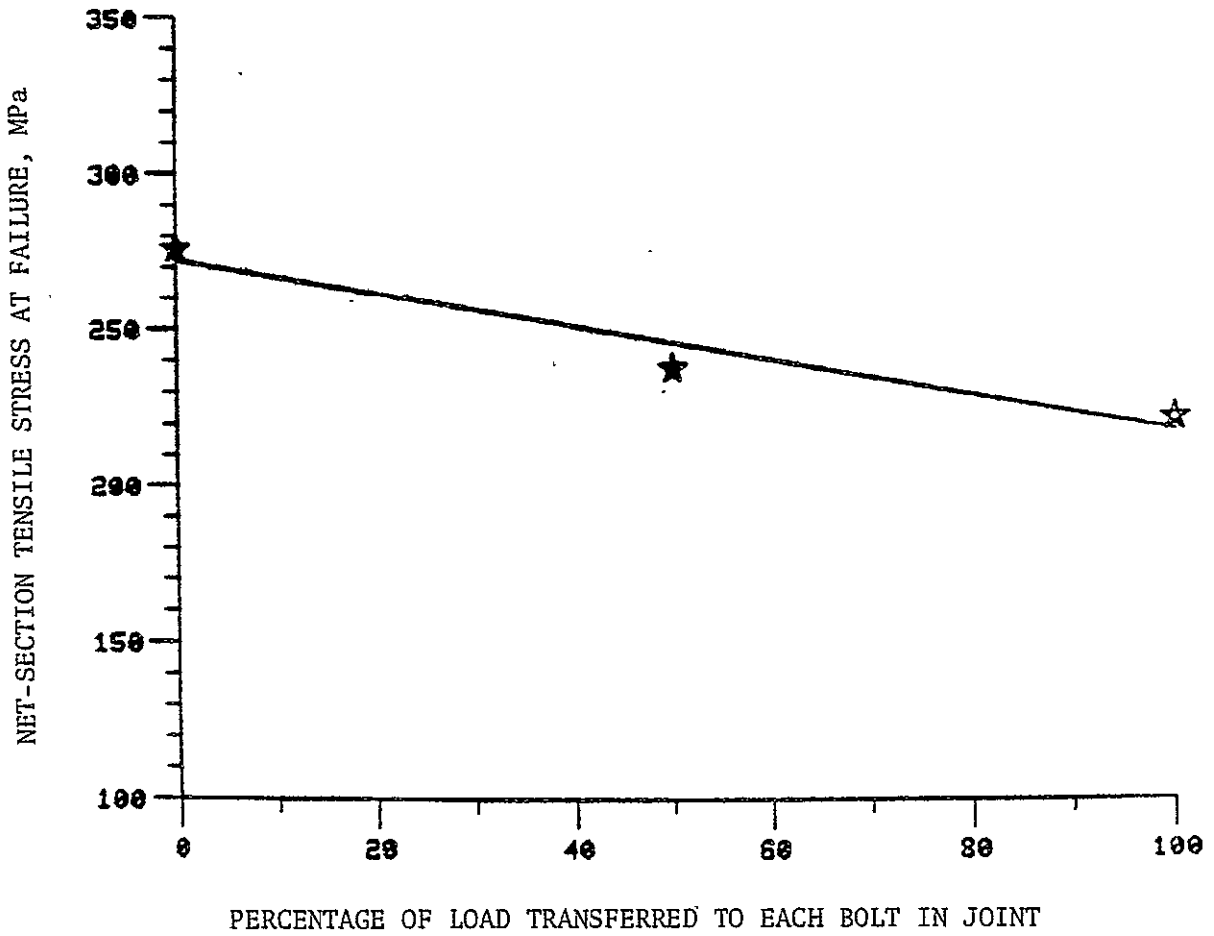
Figure 24.   Effect of the number of bolts on load-carrying capacity,
             group A3, averaged data.

Figure 25. Effect of the number of bolts on load-carrying capacity, group A4, averaged data.
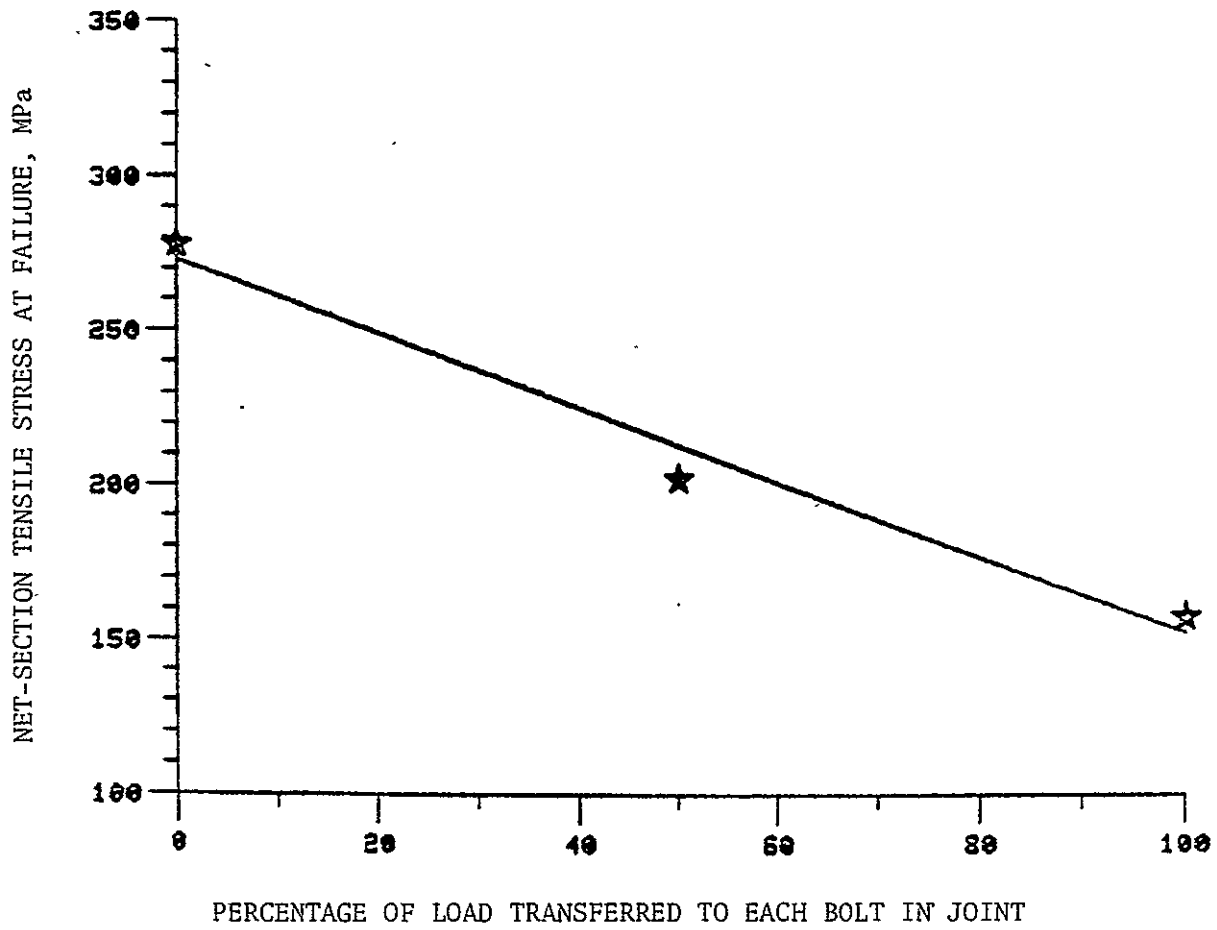
Figure 26. Effect of the number of bolts on load-carrying capacity, group A5, averaged data.

Figure 27. Effect of the number of bolts on load-carrying capacity,
group A6, averaged data.

Figure 28. Effect of the number of bolts on load-carrying capacity, group B1, averaged data.

Figure 29. Effect of the number of bolts on load-carrying capacity, group B2, averaged data.

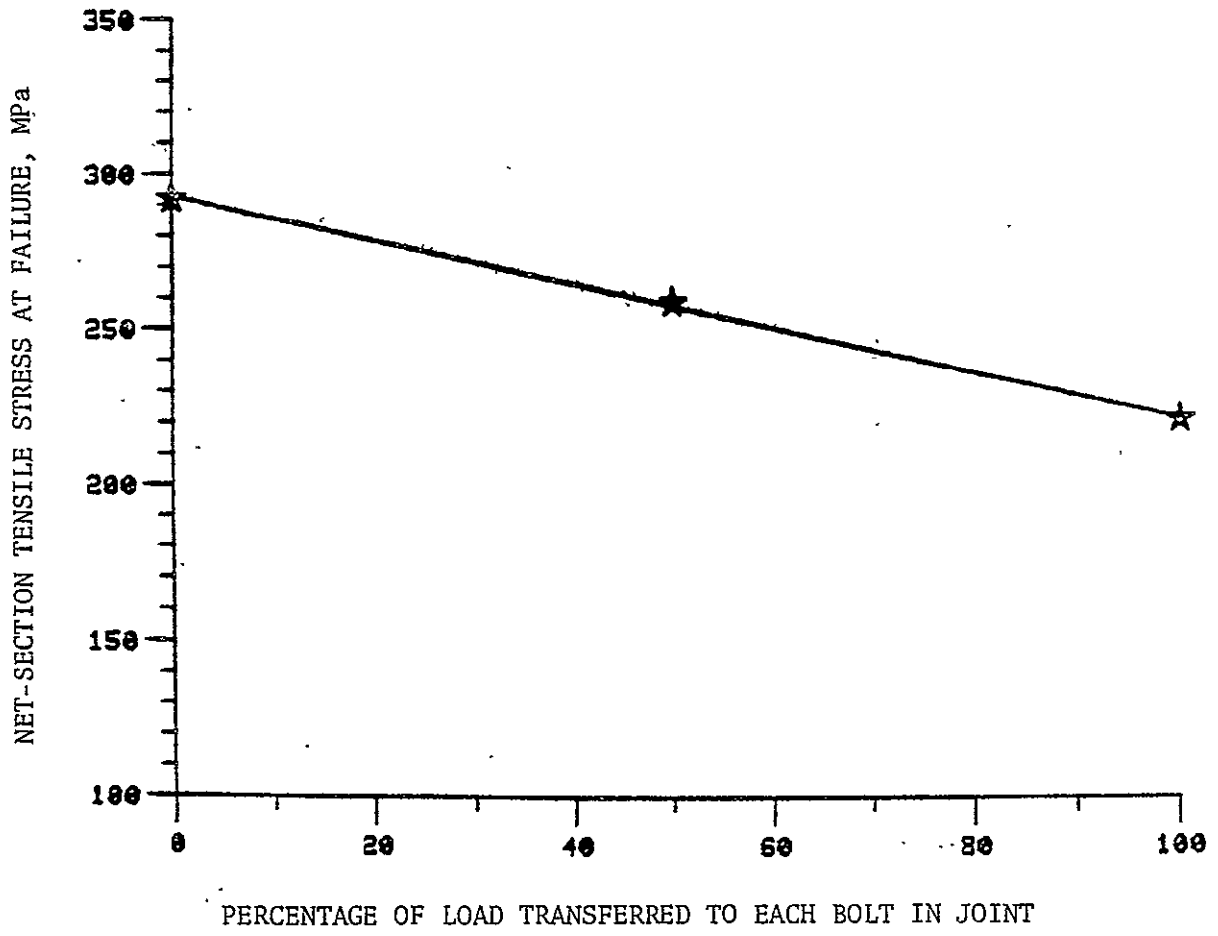Figure 30. Effect of the number of bolts on load-carrying capacity, group B3, averaged data.

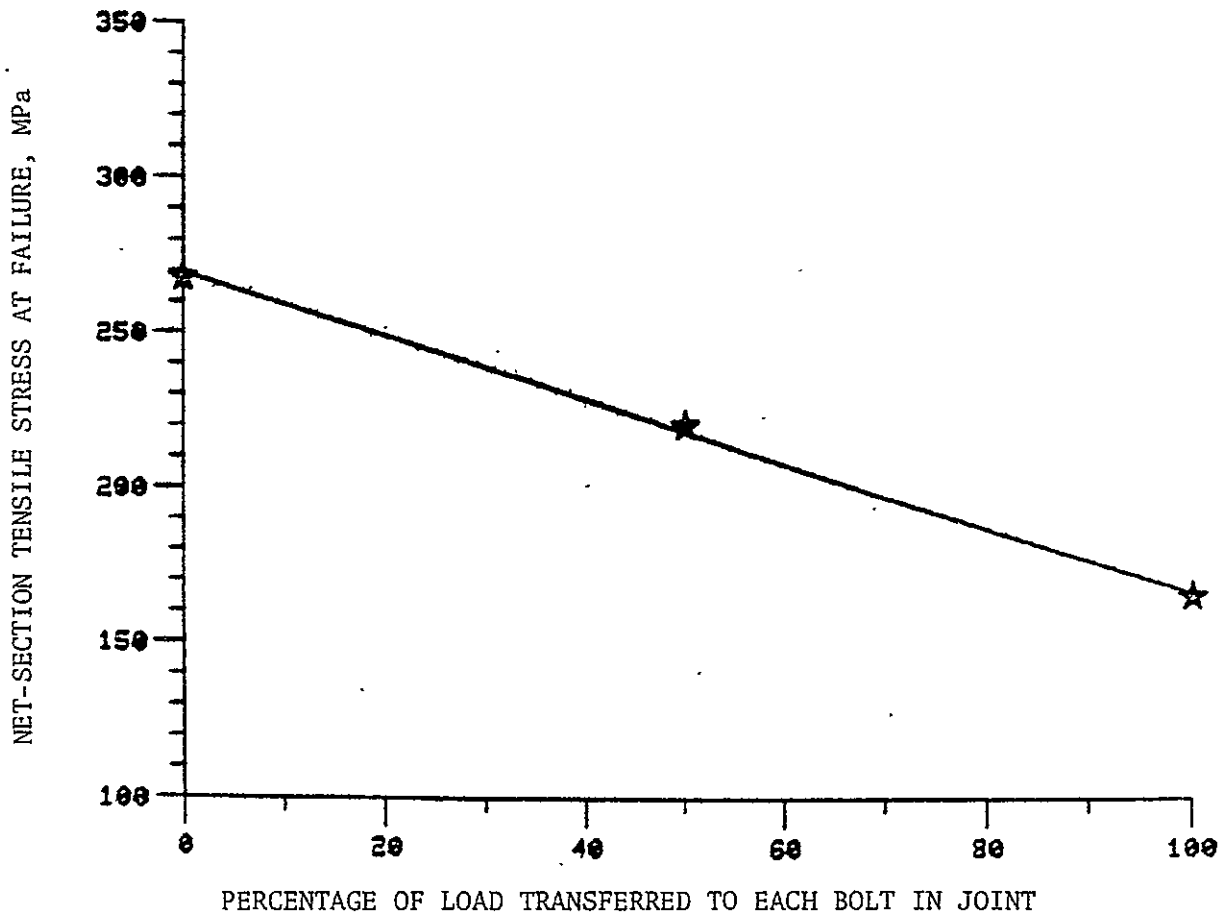Figure 31. Effect of the number of bolts on load-carrying capacity, group B4, averaged data.

Figure 32. Effect of the number of bolts on load-carrying capacity, group B5, averaged data.
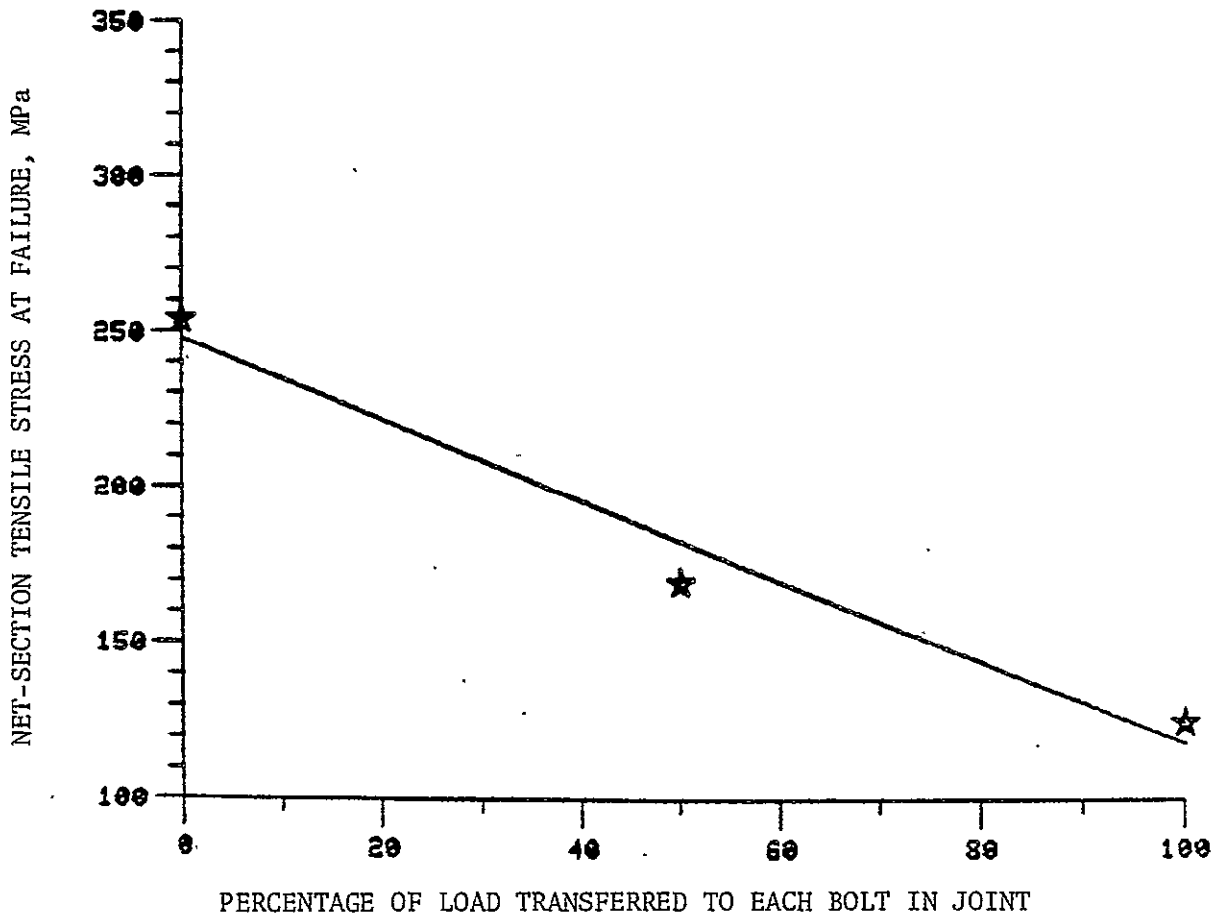
Figure 33. Effect of the number of bolts on load-carrying capacity, group B6, averaged data.